Compound soil and atmospheric drought events and CO2 fluxes of a mixed deciduous forest: Occurrence, impact, and temporal contribution of main drivers

Author(s):
Scapucci, Liliana; Shekhar, Ankit; Aranda-Barranco, Sergio; Bolshakova, Anastasiia; Hörtnagl, Lukas; Gharun, Mana; Buchmann, Nina

Publication date:
2024-02-26

Permanent link:
https://doi.org/10.3929/ethz-b-000663443

Originally published in:
EGUsphere, https://doi.org/10.5194/egusphere-2024-459

Funding acknowledgement:
ETH-27 19-1 - Forest Vulnerability to Extreme and Repeated Climatic Stress (FEVER) (ETHZ)
197357 - COS and below-canopy CO2 fluxes of two Swiss forests: understanding land-atmosphere ecosystem exchange (COCO) (SNF)
198227 - ICOS-CH Phase 3 (SNF)
198094 - Unravel the changing contributions of abiotic vs. biotic drivers of ecosystem gas exchange under weather extremes (SNF)

https://doi.org/10.5194/egusphere-2024-459
Preprint. Discussion started: 26 February 2024

Compound soil and atmospheric drought events and CO_2 fluxes of a mixed deciduous forest: Occurrence, impact, and temporal contribution of main drivers

Liliana Scapucci[1,*,♦], Ankit Shekhar[1,♦], Sergio Aranda-Barranco[2], Anastasiia Bolshakova[3], Lukas Hörtnagl[1], Mana Gharun[4], Nina Buchmann[1]

[1] Department of Environmental Systems Science, ETH Zürich, Switzerland
[2] Department of Ecology, University of Granada, Granada, Spain
[3] University of Natural Resources and Life Sciences, Vienna (BOKU), Austri
[4] Department of Geosciences, University of Münster, Germany

Correspondence to: Liliana Scapucci (liliana.scapucci@usys.ethz.ch)

♦Both the authors contributed equally to the manuscript

Abstract. With global warming, forests are facing an increased exposure to compound soil and atmospheric drought (CSAD) events, characterized by low soil water content (SWC) and high vapor pressure deficit (VPD). Such CSAD events trigger responses in both ecosystem and forest floor CO_2 fluxes, of which we know little about. In this study, we used multi-year daily and daytime above canopy (18 years; 2005-2022) and daily forest floor (five years; 2018-2022) eddy-covariance CO_2 fluxes of a Swiss forest site (montane mixed deciduous forest; CH-Lae). The objectives were (1) to characterize CSAD events at CH-Lae; (2) to quantify the impact of CSAD events on ecosystem and forest floor daily CO_2 fluxes; and (3) to identify the major drivers and their temporal contributions to changing ecosystem and forest floor CO_2 fluxes during CSAD events and CSAD growing seasons. Our results showed that the growing seasons of 2015, 2018, and 2022, were the top three driest (referred as CSAD years) at CH-Lae since 2005, with similar intensity and duration of the respective CSAD events, but considerably different pre-drought conditions. The CSAD events reduced daily mean net ecosystem productivity (NEP) in all three CSAD years, with highest reduction during 2022 (30% decrease). This reduction in daily mean NEP was largely due to decreased gross primary productivity (GPP; >15% decrease) rather than increased ecosystem respiration (Reco) during CSAD events. Furthermore, forest floor respiration (Rff) decreased during the CSAD events in 2018 and 2022 (no measurements in 2015), with a larger reduction in 2022 (>40%) than in 2018 (<25%) compared to the long-term mean (2019-2021). Using data-driven machine learning methods, we identified the major drivers of NEP and Rff during CSAD events. While daytime mean NEP during 2015 and 2018 CSAD events was limited by VPD or SWC, respectively, daytime mean NEP during the 2022 CSAD event was strongly limited by both SWC and VPD. Air temperature always had always negative effects, net radiation positive effects on daytime mean NEP during all CSAD events. Daily mean Rff during the 2018 CSAD event was driven by soil temperature and SWC, but severely limited by SWC during the 2022 CSAD event. We found that a multi-layer analysis of

https://doi.org/10.5194/egusphere-2024-459
Preprint. Discussion started: 26 February 2024

CO_2 fluxes in forests is necessary to better understand forest responses to CSAD events, particularly if the first signs we saw of acclimation to such CSAD events for our forest are found elsewhere as well. We conclude that such events have multiple drivers with different temporal contributions, making prediction of site-specific CSADs and forest long-term responses to such conditions more challenging.

1 Introduction

Forests play an essential role in mitigating climate change thanks to their ability to partially offset anthropogenic CO_2 emissions (Harris et al., 2021). However, the increasing frequency of droughts and heatwaves is compromising the carbon uptake capacity of forests worldwide (Anderegg et al., 2022). According to IPCC (2022), the temperature increase over Europe (1850-1990) has been about twice the global mean since the pre-industrial period, accompanied with an increase in frequency of drought events (Spinoni et al., 2018). Recent studies have revealed that European forests are showing increasing rates of tree mortality, induced by low soil water content (SWC) (George et al., 2022). In addition, recent studies have highlighted the role of high vapor pressure deficit (VPD), an indicator of atmospheric drought and a distinct characteristic of heatwaves, in further exacerbating tree mortality (Birami et al., 2018; Gazol and Camarero, 2022; Grossiord et al., 2017, 2020). Due to enhanced land-atmosphere feedback due to climate change, the frequency of co-occurrence of low soil moisture and high VPD has also increased (Dirmeyer et al., 2021; Miralles et al., 2019; Orth 2021; Zhou et al., 2019), resulting in so called compound soil and atmospheric drought (CSAD) conditions. The 21st century European droughts in 2003, 2015, 2018, and the most recent one in 2022, were indeed characterized by CSAD conditions (Dirmeyer et al., 2021; Ionita et al., 2021, 2017; Lu et al., 2023; Tripathy and Mishra, 2023). In 2022, Europe experienced its hottest and driest year on record, with the summer being the warmest ever recorded, which ultimately led to numerous CSAD events across the continent (Copernicus Climate Change Service, 2023).
Such CSAD events have multiple impacts on forest ecosystems. They can lead to reduced net ecosystem productivity (NEP) by decreasing gross primary productivity (GPP) and/or increasing ecosystem respiration (Reco) (Xu et al., 2020). Additionally, soil respiration (SR) can be reduced due to water scarcity in the soil, which limits both heterotrophic and autotrophic respiration (Ruehr and Buchmann, 2009; Ruehr et al., 2010; van Straaten et al., 2011; Sun et al., 2019; Schindlbacher et al., 2012). Still, high soil temperature (TS) can increase SR rates when soil moisture is not limiting metabolic reactions in the soil (Schindlbacher et al., 2012), affecting the sensitivity of respiration to soil temperature (Sun et al., 2019). The summer of 2022 in Europe, characterized by CSAD conditions (Tripathy and Mishra, 2023; van der Woude et al., 2023), showed an extensive reduction in forest greenness (about 30% of temperate and Mediterranean European forest area; Hermann et al., 2023), and a reduction in GPP (van der Woude et al., 2023), comparable to summer 2018 CSAD events. In 2018, this resulted in drought-induced tree mortality in Scots pine (*Pinus sylvestris* L.) and European beech (*Fagus sylvatica* L.) forests (Haberstroh et al., 2022; Obladen et al., 2021; Rukh et al., 2023; Schuldt et al., 2020). Clearly, most drought impact studies use data measured above the canopy, be it net carbon dioxide (CO_2) exchange or remote sensing of vegetation, particular the latter largely neglecting the below canopy component of the forest (also known as forest floor), which might show contrasting responses to

https://doi.org/10.5194/egusphere-2024-459
Preprint. Discussion started: 26 February 2024

drought conditions (Chi et al., 2021). The forest floor, composed of soil, tree roots, woody debris, and understory vegetation, provides an essential interface for soil-atmosphere CO_2 exchange, with photosynthesis of understory vegetation and forest floor respiration (Rff), both representing major CO_2 exchange pathways (Chi et al., 2017; Paul-Limoges et al., 2017). Therefore, separating the ecosystem-level drought response from the forest floor drought response provides a more comprehensive insight into drought impacts than one level alone (Chi et al., 2017; Martinez-Garcia et al., 2022). Furthermore, the intensity and duration of CSAD events, and their impacts on forests can largely vary at regional scale (Pei et al., 2013; Kim et al., 2020). Thus, more attention is needed on temperate forest ecosystems across Central Europe, such as in Switzerland, where forests are accustomed to humid and cool climates, with ample amount of summer rainfalls (Schuldt and Ruehr, 2022). In Switzerland, 2022 was the warmest year on record since the beginning of instrumental measurements in 1864, with average air temperatures 1.6 °C above the long-term mean (1991-2020), and annual precipitation amounting to only 60% of the long-term average (MeteoSvizzera, 2023). Such hot and dry conditions as in 2022 were bound to result in CSAD events which could ultimately compromise the carbon dioxide uptake capacity of forests. Thus, the objectives of this study were as follows: (1) to characterize compound soil and atmospheric drought (CSAD) events at a Swiss montane mixed deciduous forest site, (2) to quantify the impact of CSAD events on ecosystem and forest floor CO_2 fluxes, and (3) to identify the major drivers of ecosystem and forest floor CO_2 fluxes and their temporal contributions during CSAD events and CSAD growing seasons.

2 Material and methods

2.1 Forest site

The study was conducted in a managed mixed deciduous mountain forest (CH-Lae at 682 m a.s.l.) located at the Lägeren, in the far east of the Jura Mountain range in Switzerland. The CH-Lae forest has a complex canopy structure with a rather high species diversity, the dominant species are European beech (*Fagus sylvatica*, 40% cover), ash (*Fraxinus excelsior*, 19% cover), Sycamore maple (*Acer pseudoplatanus*, 13% cover), European silver fir (*Abies alba*, 8% cover), large-leaved linden (*Tilia platyphyllos*, 8%) and Norway spruce (*Picea abies*, 4% cover) (Paul-Limoges et al., 2020). The soils at CH-Lae are characterized by two main types, rendzic leptosols and haplic cambiosols, with bedrocks of limestone marl, sandstone, and transition zones between the two (Ruehr et al., 2010). The mean annual temperature at CH-Lae was 8.8 ± 1.3 °C (mean ± sd), and mean annual precipitation was 831 ± 121 mm (mean 2005-2022). The understory vegetation at CH-Lae is dominated by wild garlic (*Allium ursinum*, height ~ 30 cm) which grows for a short period in spring and early summer (March-June) (Ruehr and Buchmann, 2009). The net carbon uptake period of CH-Lae is from May to September (Figure A1, appendix A).

2.2 Ecosystem-level measurements

Measurements of ecosystem CO_2 fluxes above the canopy using the eddy covariance (EC) technique (Aubinet et al., 2012) started in April 2004. Here we used data from 2005 to 2022 (full years) of net ecosystem productivity (NEP), gross primary productivity (GPP), and ecosystem respiration (Reco). The EC system (eddy tower coordinates: 47°28'42.0" N and 8°21'51.8"

https://doi.org/10.5194/egusphere-2024-459
Preprint. Discussion started: 26 February 2024

E) was mounted at a height of 47 m (mean canopy height of 30 m). We performed high frequency (20 Hz) measurements of wind speed and wind direction using a three-dimensional sonic anemometer and used an infrared gas analyser (IRGA) to measure CO_2 molar density (with open-path IRGA from 2004-2015) or dry mole fraction (closed-path IRGA from 2016-2022; for details of instrumentation used in the EC system, see Table A1, appendix A). The time-lag between turbulent fluctuations of vertical wind speed and CO_2 molar density or dry mole fraction was calculated by covariance maximization (Fan et al., 1990), and half-hourly fluxes of CO_2 (F_C, µmol CO_2 $m^{-2}s^{-1}$) were then calculated from the 20 Hz measurements using the EddyPro software v7 (v7.0.9, LI-COR Inc., Lincoln, NE, USA), following established community guidelines (Aubinet et al., 2012; Sabbatini et al., 2018). Fluxes from the open-path IRGA LI-7500 were corrected for air density fluctuations (Webb et al., 1980). Spectral corrections for high-pass (Moncrieff et al., 2004) and low-pass filtering (Fratini et al., 2012; Horst, 1997) losses were applied to the raw fluxes. The impact of self-heating of the open-path IRGA on F_C was corrected following the method described by Kittler et al. (2017). Thereafter, F_C were filtered for turbulent conditions based on the steady state test statistic and integrated turbulence criterion test (Foken et al., 2004). Additional quality control flags (QCF) for each half-hourly CO_2 flux were calculated based on Sabbatini et al. (2018); fluxes with QCF=2 (unreliable flux value) were removed. The net ecosystem exchange (NEE) was then calculated as the sum of F_C and the CO_2 storage term. Thereafter, four quality checks were applied to the calculated NEE, namely (1) despiking using a Hampel filter to reject NEE values higher or lower than five times the standard deviation from the median absolute deviation in a 9-day running window, (2) absolute threshold filtering to remove values outside a physically plausible range of -50 to 50 µmol $m^{-2}s^{-1}$, (3) removal of potential non-biotic fluxes during cold season using a trimming mean approach (see Etzold et al., 2011), (4) constant u* (friction velocity) filtering of 0.3 ms^{-1} for CH-Lae (Etzold et al., 2010). Then, the missing and filtered NEE time series was gap-filled using the marginal distribution sampling (MDS) approach as implemented in the *ReddyProc* v1.3.2 R-package (Reichstein et al., 2005; Wutzler et al., 2018). Finally, the gap-filled NEE was partitioned into GPP and Reco using the day-time partitioning method (Lasslop et al., 2010). In this study, we used net ecosystem productivity (NEP = -NEE) for further data analyses. Positive NEP fluxes represent CO_2 uptake by the forest, whereas negative NEP represent CO_2 release. Along with fluxes, we also measured half-hourly air temperature (Tair), relative humidity (RH), incoming short-wave radiation (Rg) and precipitation (Precip) at the top of the EC tower from 2005-2022 (see Table A1 for instrumentation details). We estimated half-hourly VPD from half-hourly measurements of air temperature and relative humidity. For more information about the processing chain refer to Shekhar et al., 2024.

2.3 Forest floor measurements

We measured forest floor fluxes of CO_2 based on the EC technique (Aubinet et al., 2012) below the canopy from 2018 to 2022 to estimate net ecosystem exchange of the forest floor (NEE_{ff}), which includes CO_2 fluxes from the soil and understory vegetation. We partitioned NEE_{ff} into gross primary productivity of the forest floor (GPP_{ff}) and respiration of the forest floor (Rff; Lasslop et al., 2010). The below-canopy station at CH-Lae site was located in a distance of c. 100 m from the main tower (47°28'42.9" N and 8°21'27.6" E) and has a height of 1.5 m. Wind speed and direction were measured with a sonic anemometer

https://doi.org/10.5194/egusphere-2024-459
Preprint. Discussion started: 26 February 2024

and CO_2 concentrations with an open-path IRGA (LI-7500; Table A1) at a frequency of 20 Hz. We calculated NEE_{ff}, and the partitioned fluxes, using the same process and corrections as for above canopy measurements, (except for the self-heating correction). We used a seasonal u* filtering to account for changes in the canopy, with 0.024 ms^{-1} for spring (day 60-151), 0.027 ms^{-1} for summer (day 152-243), 0.039 ms^{-1} for autumn (day 244-334), and 0.025 ms^{-1} for winter (day 335-60). Additionally, we continuously measured air temperature ($Tair_{ff}$), relative humidity (RH_{ff}), incoming short-wave radiation (Rg_{ff}), soil temperature (TS) and soil water content (SWC) at multiple depths at the forest floor meteorological station next to the below-canopy EC system (Table A1, appendix A). In 2020, we installed an additional soil moisture profile. To account for spatial heterogeneity, we centre-normalised the SWC data and used z-scores of SWC for further analyses.

2.4 Soil respiration measurements

Ten PVC collars (diameter 20 cm, height 13 cm, depth = 2 cm) were installed at CH-Lae in spring 2022, at the same locations within the footprint of the tower as described in Ruehr et al. (2010). Soil respiration (SR) measurement campaigns were performed at least once a month from March until November 2022, with a LI-8100-103 analyser and a closed chamber (Table A1, appendix A). Collars were measured once a day in a random order during each campaign. Every measurement lasted 90 seconds from the moment the LI-8100 chamber closed on top of the collar. Next to each collar, we measured SWC_S (SWC from survey measurements) at 5 cm with a soil moisture sensor, and TS_S (TS from survey measurements) at 5 cm with a temperature sensor (Table A1, appendix A). When the Swiss meteorological service (MeteoSwiss) forecasted a two-week heatwave starting on 14th of July 2022, we intensified the measurements of SR to one campaign every second day with two rounds of measurements per day for two weeks (at 09:00 and at 16:00). The order of measurements was inverted every fieldwork day. Since the portable soil moisture sensor broke on 22nd of July 2022 and was only available on 11th of August 2022, we calculated the SWC based on continuous measurements at the forest floor meteorological station for these days ($SWCs = 1.34 * SWC - 10.7$; $R^2 = 0.82$).

2.5 Data analyses

In this study, we focused all our analysis on the growing season, between May and September, when the long-term mean of ecosystem NEP (2005-2022) was positive, implying that GPP of the vegetation overcompensated all respiratory losses (Figure A1, appendix A; Körner et al., 2023). We conducted all data analyses using R programming language (R core team, 2021). We compared cumulative precipitation (indicating total water supply to the forest) and cumulative VPD (indicating total atmospheric water demand) during the growing seasons of 18 years at our forest site and chose the three years with the driest growing seasons i.e., with low cumulative precipitation and high VPD. Then, we identified the CSAD events during the CSAD years as periods when both soil and atmosphere were significantly drier than usual for more than 10 consecutive days, implying a compound drought condition. To identify drier than usual periods, we compared 5-day moving daily means (assigned to the centre of 5 days) of SWC and VPD with their long-term (2005-2022) means. So, a period of 10 or more consecutive days with

https://doi.org/10.5194/egusphere-2024-459
Preprint. Discussion started: 26 February 2024

SWC being significantly lower ($p<0.05$) and VPD being significantly higher ($p<0.05$) than the long-term mean, were identified as CSAD events.

We quantified the impact of CSAD events based on anomalies of NEP, GPP, Reco, and Rff by comparing them with their respective long-term means (NEP, GPP, Reco: mean of 2005-2022; Rff: mean of 2019-2021). Since CSAD events occurred in two of the five years of flux data available at the forest floor station (Rff), we excluded 2018 and 2022 from the calculation of long-term mean. To understand the major drivers of NEP and Rff, we performed two different driver analyses in this study, first focusing on the CSAD years, and second focusing on the CSAD events in the CSAD years.

(I) For the first driver analysis, we used the conditional variable importance (CVI) feature based on random forest regression model (Breiman, 2001). For modelling daily mean NEP, the predictors were Rg, VPD, and Tair measured above the canopy, and SWC measured at the forest floor station, whereas for modelling daily mean Rff, the predictors were Rg (Rg_{ff}) and Tair ($Tair_{ff}$) as well as soil temperature (TS) and SWC, measured at the forest floor station. The CVI considers the multi-collinearity between the predictors (i.e., Tair, VPD, Rg), while estimating the importance of predictor variables. For estimating CVI, we used the *cforest* and *varimp* function from the R-package *party* (Hothorn et al., 2006).

(II) For the second driver analysis, we used daytime mean NEP (excluding nighttime data) to avoid potential biases if GPP were used since some predictors, i.e., Tair and Rg, were used for the partitioning of NEE into GPP and Reco. We used a TreeExplainer-based SHapley Additive exPlanations (SHAP) framework (Lundberg and Lee, 2017; Lundberg et al., 2020), with a tree-based ensemble learning extreme gradient boosting (XGB) model (Chen and Guestrin, 2016). The XGB model was used to model daytime mean NEP and daily mean Rff, applying the GridSearchCV methodology to optimize the parameters of the XGB model for NEP and Rff (see Wang et al., 2022 for more details). The TreeExplainer-based SHAP framework integrates explanatory models (here the XGM model) with game theory (Shapley, 1953) which allowed us to estimate the marginal contribution (known as SHAP value) of each predictor variable (i.e., Tair, VPD, SWC, TS) to predicted response variables. We used the function *xgboost* (eXtreme Boosting Training) from the R-package *xgboost* to train the model, and the functions *shap.values* and *shap.prep* from the R-package *SHAPforxgboost* (Chen and Guestrin, 2016) to obtain the SHAP values of each predictor variable for daytime mean NEP (for 2005-2022) and daily mean Rff (for 2018-2022). Then we calculated the mean SHAP value during the CSAD events for each predictor of daytime mean NEP and daily mean Rff for the CSAD years. For comparison, we also calculated the mean SHAP values of the predictors during the respective reference periods (long-term means: 2005-2022 for daytime mean NEP; 2019-2021 for daily Rff). The respective reference period includes all days in which a CSAD event occurred independent of the year, i.e., ranging from 7th July to 23rd August for daytime mean NEP during 2005-2022 (including CSAD years due to the large number of years available with measurements), and from 14th July to 23rd August for daily mean Rff during 2019-2021 (excluding CSAD years due to the small number of years available with measurements; Figure A2, appendix A).

Moreover, we used SHAP values of drivers (VPD, Tair and SWC for NEP; TS and SWC for Rff) to derive driver thresholds, i.e., the absolute driver values related to largest effects as indicated by highest marginal contributions to the response variables NEP and Rff for each CSAD year (Gou et al., 2023; Wang et al., 2022). For this, we fitted a local polynomial regression

https://doi.org/10.5194/egusphere-2024-459
Preprint. Discussion started: 26 February 2024

(LOESS curve) between the SHAP values of the driver variable and the driver variable itself, and then identified the absolute driver value corresponding to the highest SHAP value. We specifically derived VPD_NEP_{max}, $Tair\_NEP_{max}$, SWC_NEP_{max}, i.e., VPD, Tair and SWC, associated with highest marginal contributions to daytime mean NEP, and TS_Rff_{max} and SWC_Rff_{max}, i.e., TS and SWC, associated with highest marginal contributions to daily mean Rff for each CSAD year. Finally, we used linear models to explain daily mean SR responses to TS and SWC during the CSAD events and the rest of the years, based on the measurements from the survey campaigns in 2022. The amount of data was not sufficient to use machine learning approaches.

3 Results

3.1 Detected CSAD events

The growing seasons (May to September) of 2015, 2018, and 2022 were the three driest in the last 18 years (2005-2022) which the mountain forest site experienced (Figure 1). The growing seasons in these three years were characterized by very high atmospheric drought (indicated by cumulative VPD) and low water supply (indicated by cumulative precipitation, a proxy for soil drought), called compound soil and atmospheric drought (CSAD) years hereafter. In particular, the summer months (June-August) of these three years were significantly warmer and drier (Figures 1, 2). Mean summer temperatures of 2018 (19.8 °C) and 2022 (20.3 °C) were more than 2.5 °C higher than the long-term mean summer temperature at the forest site (17.2 °C); summer precipitation sums in 2018 and 2022 were more than 20% and 10% lower than the long-term mean cumulative summer precipitation (300 mm), respectively. Furthermore, during the month July of both years 2015 and 2022, less than one-third of long-term mean cumulative summer precipitation was recorded. Coupled with a more than 50% increase in average VPD this resulted in intense soil and atmospheric drought conditions.

Moreover, we detected two distinct CSAD events in 2015, i.e., periods of 10 or more consecutive days with significantly lower SWC and significantly higher VPD than the long-term mean: one from 7th July 2015 to 21st July 2015, and a second one from 2nd August 2015 to 13th August 2015 (Figure 2a, d, g), comprising a total of 25 days with a mean maximum temperature of 26.9 °C, mean maximum VPD of 2.24 kPa, and mean minimum normalized SWC of -1.83 (Table 1). For comparison, in 2018, the CSAD event lasted for 31 days, from 23rd July 2018 to 23rd August 2018 (Figure 2b, e, h), with a mean maximum temperature of 27.7 °C, mean maximum VPD of 2.19 kPa, and mean minimum normalized SWC of -1.94 (Table 1). In 2022, the CSAD event lasted 21 days, from 14th July 2022 to 4th August 2022. Thus, although it was shorter than in those in 2015 and 2018 (Figure 2c, f, i), it more intense than those in 2015 and 2018, with mean maximum temperature of 28.3 °C, mean minimum VPD of 2.43 kPa, and mean minimum normalized SWC of -2.51 (Table 1). We measured the highest air temperature (33.56 °C) and the third highest VPD (3.83 kPa) ever recorded at the forest site in the past 18 years (2005-2022) on the last day of the 2022 CSAD event, i.e., on 4th August 2022 between 16:30 and 17:00 (Figure A3, appendix A). Furthermore, the 2022 CSAD event was characterized by multiple tropical nights (i.e., nighttime temperature > 20 °C; Figure A3, appendix A) and progressive soil drying (Figure 2).

https://doi.org/10.5194/egusphere-2024-459
Preprint. Discussion started: 26 February 2024

Thus, the CSAD events were not only slightly different in terms of intensities, but also in terms of time of CSAD occurrence (Table 1), and initial drought development. In both years 2015 and 2018, wetter (than long-term mean; 2015) or normal (2018) soil conditions continued from late spring (mid-May) until end of June, with a quick soil drought intensification in July due to high air temperatures (> 30°C), high VPD (>3.8 kPa) (Figure 2), and low precipitation (more than 40% lower than the long-term July average). The year 2022, however, was already characterized by exceptionally low soil water content and high VPD (> 2.5 kPa) in May (Figure 2i), which intensified with low precipitation and high temperatures into early summer. Nighttime VPD exceeded 2 kPa on a few days in June, before the CSAD event occurred mid-July to beginning of August (see Figure A3, appendix A). Even the heavy rainfall on 5th August 2022 (28 mm) only resulted in a minor increase of SWC. Nevertheless, after 4th August, air temperature and VPD conditions became near-normal, thereby marking the end of the 2022 CSAD event (Figure 2).

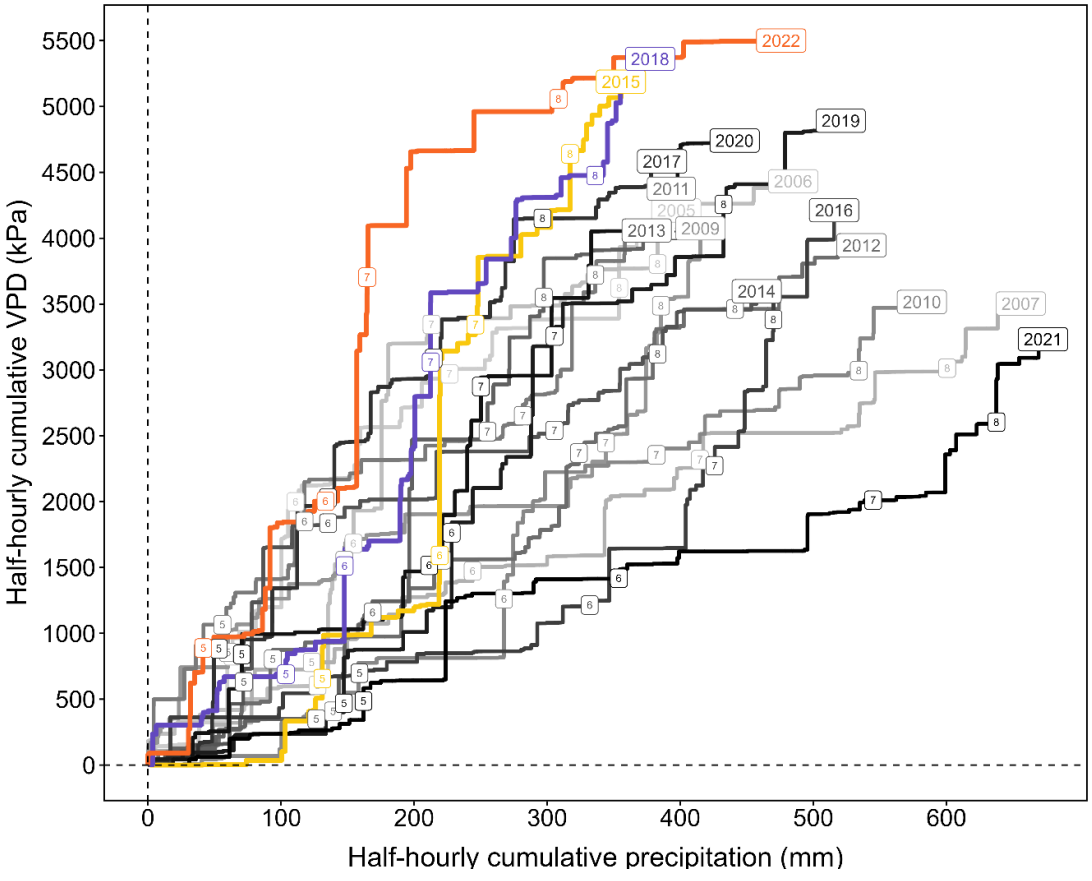

Figure 1. Cumulative VPD and cumulative precipitation from May to September (growing season of the Lägeren forest) of each year (2005-2022). The numbers (5-9) on the cumulative lines depict the end of each month.

https://doi.org/10.5194/egusphere-2024-459
Preprint. Discussion started: 26 February 2024

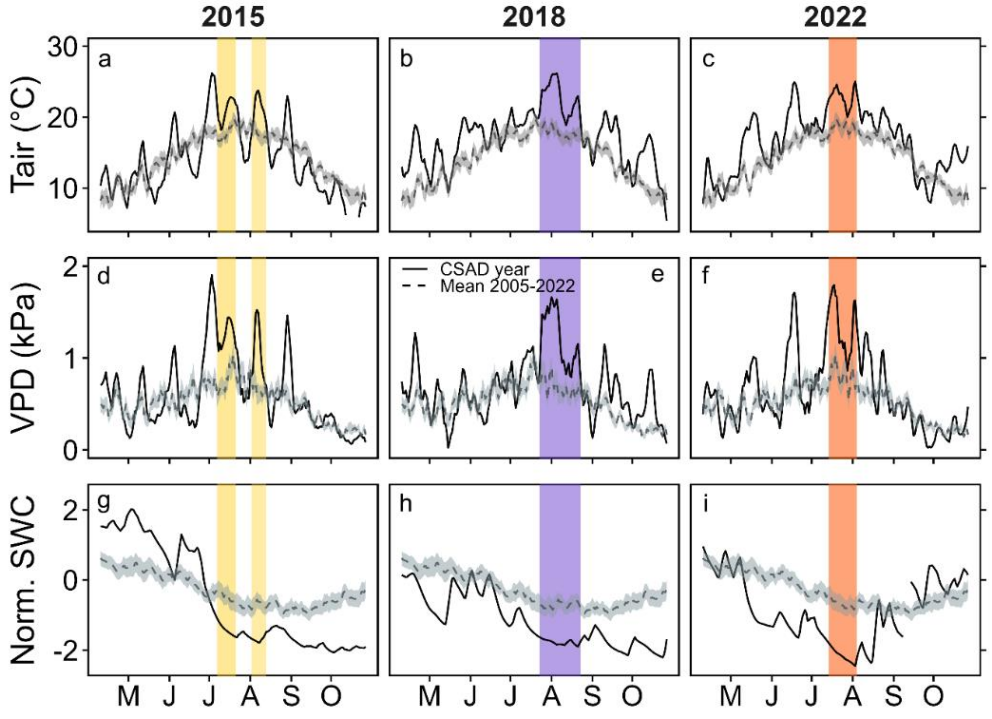

Figure 2. Comparison of 5 day moving averages of daily mean (a-c) Tair, (d-f) VPD, and (g-i) SWC in the years when a CSAD event happened against the long-term means (2005-2022). The coloured areas mark the CSAD events, i.e., periods with co-occurring lowest SWC and highest VPD.

Table 1. Characterization of CSAD events in 2015, 2018 and 2022. Duration, maximum (Max.) and standard deviation (± SD) of daily mean Tair, maximum (Max.) and standard deviation (± SD) of daily mean VPD, and minimum (Min.) and standard deviation (± SD) of daily mean normalized SWC recorded during the CSAD events in 2015, 2018 and 2022 are given.

Year	Duration (days)	Max. ± SD Tair (°C)	Max. ± SD VPD (kPa)	Min. ± SD SWC (normalized)
2015	11 + 14 = 25	26.9 ± 3.03	2.24 ± 0.4	-1.83 ± 0.20
2018	31	27.7 ± 2.88	2.19 ± 0.5	-1.93 ± 0.10
2022	21	28.3 ± 2.64	2.43 ± 0.5	-2.51 ± 0.20

3.2 Impacts of CSAD events on CO_2 fluxes

All CSAD events had immediate negative impacts on ecosystem CO_2 fluxes, showing a decrease in the CO_2 fluxes compared to the long term-means (Table 2, Figure 3a, c, e, g). Mean daily NEP, GPP, Reco and Rff tended to be lower during the CSAD events compared to the respective long-term means of the reference periods 2005-2022 (for NEP, GPP and Reco) and 2019-2021 (for Rff; Table 2), with much larger variations during CSAD events compared to those of the reference periods (except

https://doi.org/10.5194/egusphere-2024-459
Preprint. Discussion started: 26 February 2024

for Rff; Figure 3b, d, f, h). The lowest average NEP was recorded in the CSAD event of 2022, followed by NEP in the 2018 and 2015 CSAD events, while the lowest average GPP and Reco were found in the 2018 CSAD event (Table 2).

All cumulative CO_2 fluxes decreased during CSAD events in 2015, 2018 and 2022 compared to the long-term means (Figure 3b, d, f, h), with the only exception of Reco in 2022. The cumulative NEP during the CSAD events in 2015 and 2018 decreased by 34 µmol CO_2 m^{-2} s^{-1} and 26 µmol CO_2 m^{-2} s^{-1}, respectively, compared to the respective long-term means of the reference periods (2005-2022; Figure 3b). During both CSAD years 2015 and 2018, cumulative GPP and Reco decreased considerably, although cumulative GPP tended to decrease more (>40 µmol CO_2 m^{-2} s^{-1}) than Reco (>30 µmol CO_2 m^{-2} s^{-1}; Figure 3d, f). In contrast, during the CSAD event in 2022, cumulative NEP decreased by 27 µmol CO_2 m^{-2} s^{-1} compared to long-term mean (Figure 3b), due to a decrease in cumulative GPP (by 44 µmol CO_2 m^{-2} s^{-1}) and only negligible changes in Reco (Figure 3d, f). Furthermore, Rff fluxes during the 2018 and 2022 CSAD events were lower compared to the long-term mean of the reference period (2019-2021), with 23 µmol CO_2 m^{-2} s^{-1} and 32 µmol CO_2 m^{-2} s^{-1}, respectively (Figure 3h). This decrease in Rff was supported by decreasing daily mean SR rates measured in 2022 (Figure 3g).

Table 2. Daily mean CO_2 fluxes during CSAD events in 2015, 2018 and 2022 as well as their long-term means during the respective reference periods. Means and standard deviation (± SD) of net ecosystem production (NEP), partitioned gross primary productivity (GPP) and ecosystem respiration (Reco) as well as forest floor respiration (Rff) are given. The reference period for NEP, GPP and Reco represents all days between the 7th of July and the 23rd of August during 2005 and 2022; the reference period for Rff represents all days between the 14th of July and 23rd of August during 2019 and 2021. All fluxes are given in µmol CO_2 m^{-2} s^{-1}. n.a. = not available.

	NEP	GPP	Reco	Rff
CSAD 2015	2.09 ± 2.14	7.33 ± 2.54	5.05 ± 2.11	n.a.
CSAD 2018	1.99 ± 1.36	6.31 ± 1.44	4.23 ± 0.89	3.19 ± 0.68
CSAD 2022	1.89 ± 1.77	6.69 ± 1.33	5.73 ± 1.55	2.24 ± 0.20
Reference period	3.2 ± 0.82	8.77 ± 0.85	6.14 ± 0.65	3.81 ± 0.26

https://doi.org/10.5194/egusphere-2024-459
Preprint. Discussion started: 26 February 2024

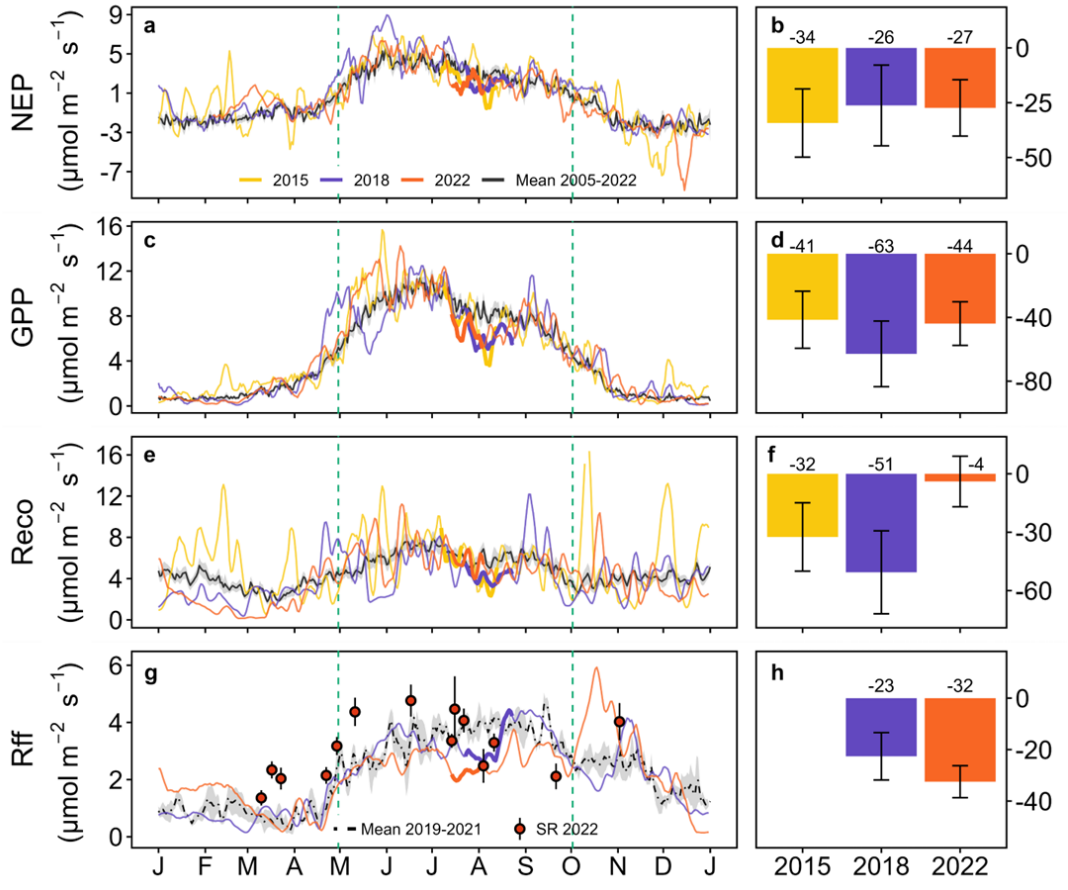

Figure 3. Comparison of daily mean (a) net ecosystem production (NEP), (b) gross primary productivity (GPP), (c) ecosystem respiration (Reco), and (d) forest floor respiration (Rff) of the years when a CSAD event occurred (2015, 2018 and 2022) against the respective long-term means (a, c, e, g). Soil respiration (SR) measurements are given as daily means (± SD) measured manually in 2022 only. Thicker lines represent CSAD events. The right panels (b, d, f, h) show the cumulative difference between the actual fluxes recorded during a CSAD event and the respective long-term mean fluxes (2005-2022 for NEP, GPP and Reco; 2019-2021 for Rff).

3.3 Drivers of NEP and Rff in 2015, 2018 and 2022

3.3.1 Comparison of drivers during the 2015, 2018, and 2022 with the long-term means

Daily mean NEP during the growing seasons in 2015 and 2018, were mainly driven by daily mean incoming solar radiation (Rg), similar to the long-term daily mean NEP during 2005-2022 (Figure 4a). However, NEP during the 2022 growing season was more strongly driven by daily mean SWC than by Rg, as indicated by its high CVI (Figure 4a). Daily mean Tair and VPD were the second most important drivers of daily mean NEP in 2015 and 2018, with a CVI higher than the ones for the long-term mean 2005-2022. Differently to NEP, daily mean Rff during the growing seasons 2019-2021 was mainly driven by daily mean SWC, followed by daily mean $Tair_{ff}$ and daily mean TS (Figure 4b). We found that daily mean SWC was the main driver

https://doi.org/10.5194/egusphere-2024-459
Preprint. Discussion started: 26 February 2024

of daily mean Rff in 2018, with a much higher CVI compared to those of other years, followed by daily mean TS. Overall, the CVI of all variables was much lower in 2022 compared to those of the other years (Figure 4b).

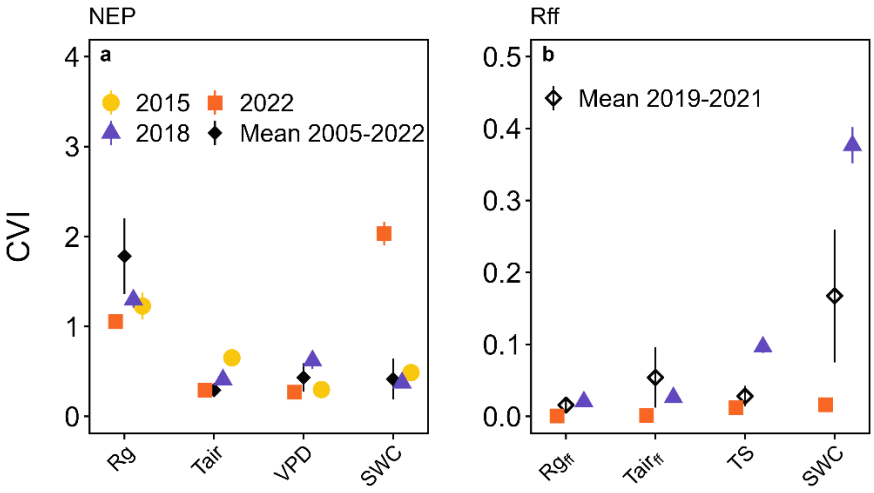

Figure 4. Driver analysis for daily mean (a) net ecosystem production (NEP) and (b) forest floor respiration (Rff) for the growing seasons 2015, 2018, 2022, compared with the daily mean NEP 2005-2022 and the daily mean Rff 2019-2021. Note: Rff was not measured in 2015. The impact of driver variables is given by their conditional variable importance (CVI), Rg (incoming solar radiation), Tair (air temperature), VPD (vapor pressure deficit) and SWC (soil water content) were considered.

3.3.2 Temporal development of important drivers of daytime NEP and daily Rff

Testing the temporal development in the main drivers of daytime NEP with SHAP analysis revealed that overall, SWC, VPD and Tair decreased NEP during all CSAD events (Figure 5), while Rg increased daytime NEP. During the two CSAD events in 2015, both Tair and VPD were always associated with a decrease in NEP, while SWC exhibited a less consistent pattern, increasing NEP during the first CSAD event and decreasing NEP during the second (Figure 5a). Nevertheless, the mean contributions of Tair, SWC and VPD to daytime mean NEP during the CSAD events of 2015 were negative, with Tair having the largest effect in reducing NEP (Figure 5a). As stated previously, Rg enhanced daytime mean NEP in both CSAD events of 2015, contributing positively to NEP (Figure 5a). During the CSAD event of 2018, the mean contributions of Tair, VPD and SWC to daytime mean NEP were also all negative, leading to a decrease in NEP (Figure 5b). In contrast to 2015, SWC showed the largest negative effect on daytime NEP during the 2018 CSAD event, although it had clear positive effects prior to the CSAD onset. Rg both enhanced and decreased daytime mean NEP during the CSAD event of 2018, which resulted in a small mean positive contribution (Figure 5b). As observed for 2018, the mean contributions of Tair, VPD and SWC were all negative during the CSAD event of 2022, leading to a decrease in NEP (Figure 5c). Similarly to 2018, prior to the 2022 CSAD, SWC had a positive effect on daytime NEP, but then contributed the most to the decrease in NEP during the 2022 CSAD. As observed previously, Rg increased daytime NEP also during the 2022 CSAD event, shown by its positive contribution (Figure 5c). Lastly, during the reference period 2005-2022 (from 7th of July to 23rd of August), Tair, VPD and SWC affected daytime NEP negatively, although the contributions of VPD and SWC were close to zero (Figure 5d). In contrast, the mean contribution of

https://doi.org/10.5194/egusphere-2024-459
Preprint. Discussion started: 26 February 2024

Rg to daytime mean NEP was positive, resulting in an increase of daytime mean NEP during the reference period 2005-2022 (Figure 5d). In accordance with the previous analysis for NEP, the decrease in daily Rff during both CSAD events of 2018 and 2022 was mainly driven by negative effects of SWC (Figure 6a, b). In contrast, TS increased Rff during both CSAD events, but with much larger effects during the CSAD in 2018 compared to that in 2022. This coincided with negative effects of SWC on Rff already starting in mid-June, one month prior to the 2018 CSAD event (Figure 6a), while during the 2022 CSAD event, SWC effects only became negative shortly before the 2022 event (Figure 6b). The effect of Rg_{ff} during both CSAD events in 2018 and 2022 was positive, but overall close to zero (Figure 6a, b). For comparison, during the reference period (from 14th of July to 23rd of August 2019-2021), TS had the largest positive effect on Rff compared to the CSAD events in 2018 and 2022, which persisted typically until September when senescence and leaf fall set in (Figure 6c). On the other hand, the effects of Rg_{ff} and SWC varied around zero throughout all reference period summers (June, July, and August) (Figure 6c). Overall, mean contributions to changes in Rff during the reference period 2019-2021 were dominated by positive effects by TS, and close to zero contributions of Rg_{ff} and SWC (Figure 6c).

https://doi.org/10.5194/egusphere-2024-459
Preprint. Discussion started: 26 February 2024

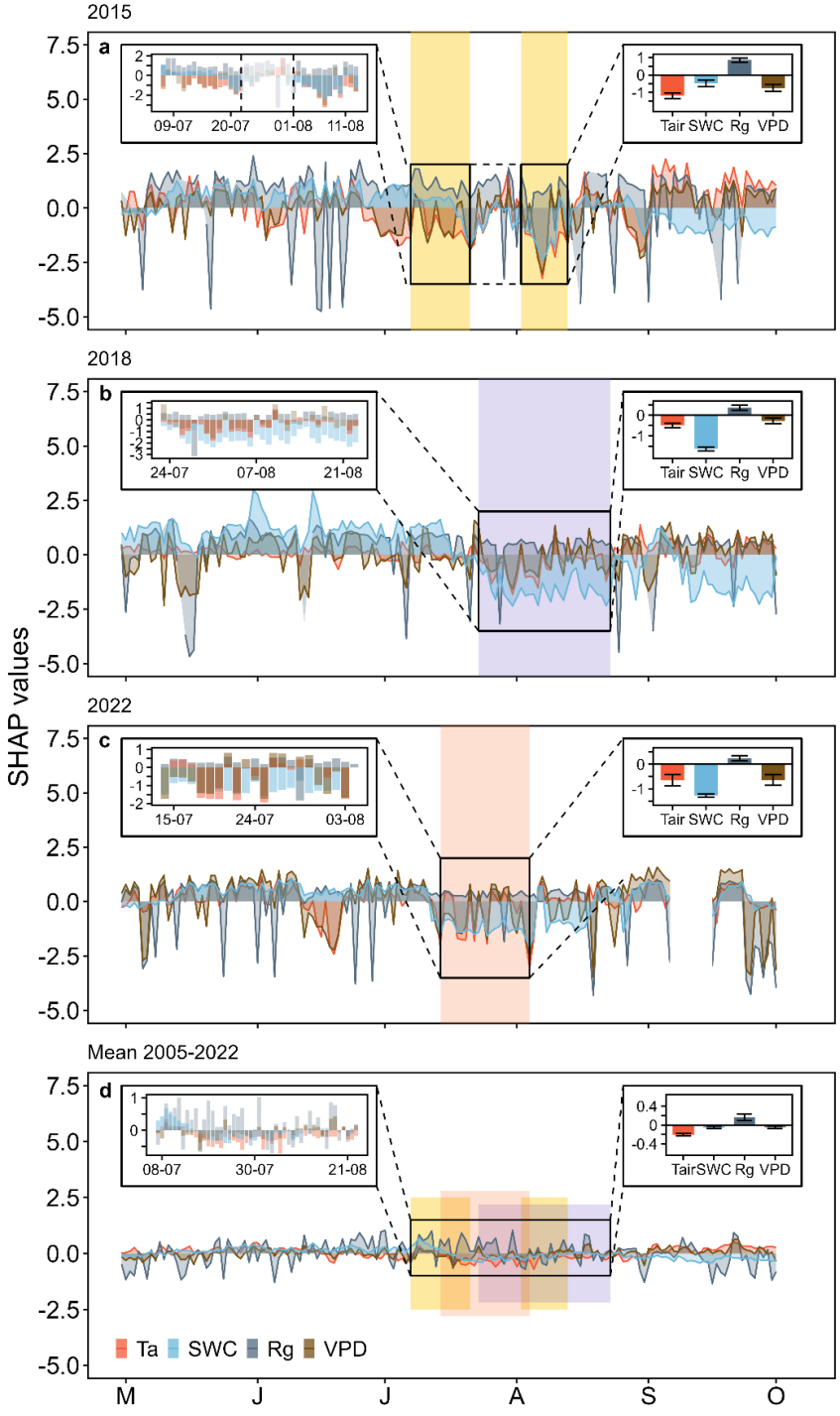

Figure 5. Temporal course of driver contributions to daytime mean net ecosystem production (NEP) during the growing seasons of (a) 2015, (b) 2018, (c) 2022, and (d) the long-term mean (2005-2022) indicated by SHAP values for Tair, incoming radiation (Rg), VPD, and SWC. The small inserts on the left show the CSAD events (a-c) and the reference period for 2005-2022 (d). The small inserts on the right show mean (± SD) SHAP values for Tair, SWC, Rg and VPD during the CSAD events (a-c) and during the

https://doi.org/10.5194/egusphere-2024-459
Preprint. Discussion started: 26 February 2024

reference period for 2005-2022 (d). Positive SHAP values indicate positive effects on the response variable NEP, while negative SHAP values indicate negative effects. Colour bands show the period in which a CSAD occurred in 2015, 2018 and 2022 (a-c); they are also shown in panel (d) to highlight the reference period for the long-term mean (2005-2022).

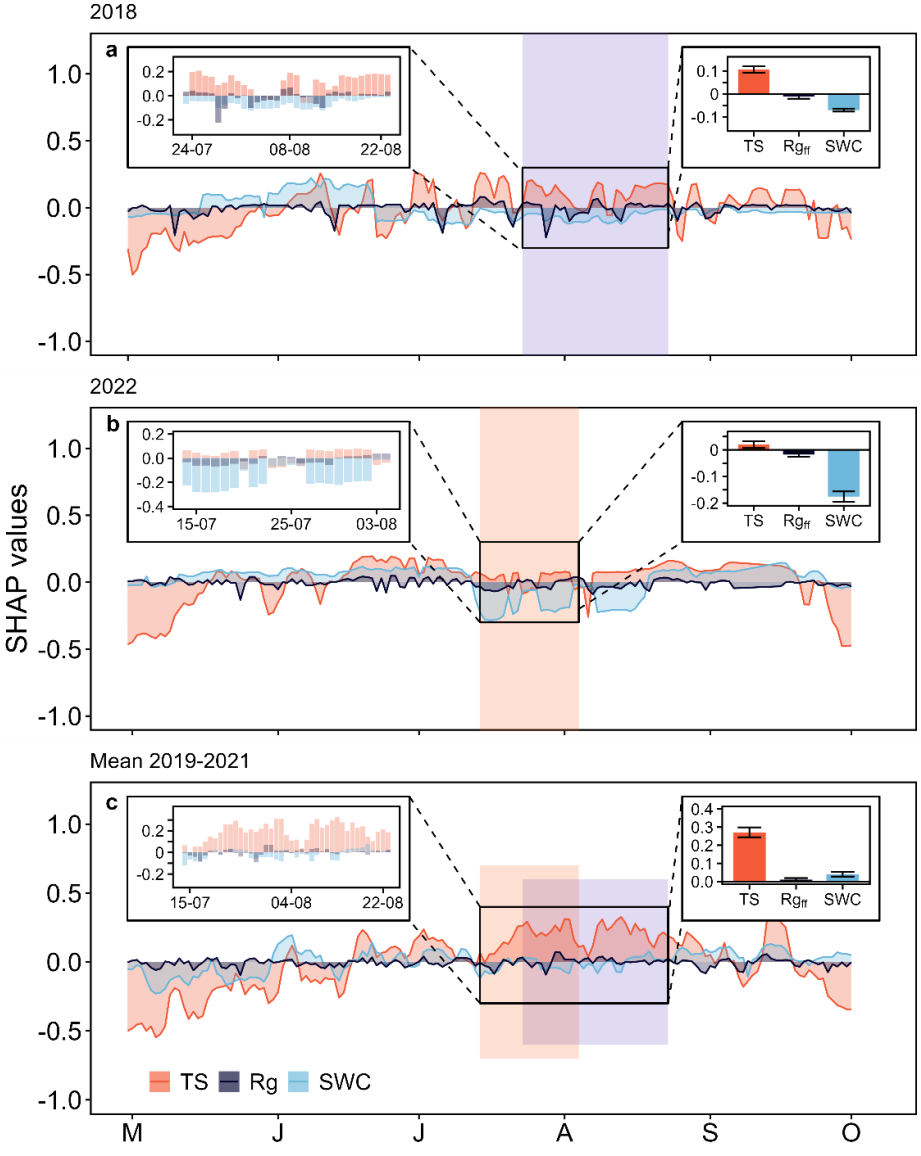

Figure 6. Temporal course of driver contributions to daily mean forest floor respiration (Rff) during the growing seasons of (a) 2018, (b) 2022, and (c) the non-CSAD years 2019-2021 indicated by SHAP values for soil temperature (TS), incoming radiation at the forest floor (Rg_{ff}), and SWC. The small inserts on the left show the CSAD events (a-b) and the reference period for 2019-2021 (from 14th July to 23rd August) (d). The small inserts on the right show mean (± SD) SHAP values for TS, Rg_{ff}, and SWC during the CSAD events (a-b) and during the reference period for 2019-2021 (c). Positive SHAP values indicate a positive effect on the response variable Rff, while negative SHAP values indicate negative effects. Colour bands show the period in which a CSAD event occurred; they are also shown in panel (c) to highlight the reference period for 2019-2021.

https://doi.org/10.5194/egusphere-2024-459
Preprint. Discussion started: 26 February 2024

3.3.3 Driver thresholds with largest effects on daytime mean NEP and daily mean Rff for the CSAD years

We derived thresholds for the drivers VPD, SWC, Tair, and TS to understand if the absolute values of these drivers during the CSAD events actually differed from the absolute values that showed largest effects on daytime mean NEP or daily mean Rff (based on the maximum marginal contributions from SHAP analysis). Threshold values differed among the CSAD years, particularly for SWC_NEP_{max} and SWC_Rff_{max} which were positive in 2015 and 2018 but negative in 2022 (Table 3). VPD_NEP_{max} were relatively low for all CSAD years (between 0.7 and 0.8 kPA), while $Tair\_NEP_{max}$ increased from around 10 °C in 2015 to 13 °C in 2018 to 16 °C in 2022. For comparison, TS_Rff_{max} were around 19 °C in 2018 and 15.6 °C in 2022. Comparing measured driver values to those thresholds revealed that most daytime mean VPD values during the CSAD events were typically higher than the respective VPD_NEP_{max} threshold for each of the CSAD years, reaching values of up to 2.5 kPA (Figure 7a, d, g), only few exceptions occurred. In contrast, all daytime mean SWC values measured during the CSAD events were far below the SWC_NEP_{max} thresholds in all CSAD years (Figure 7b, e, h), resulting in very negative effects on daytime NEP. We also observed a decrease in SWC_NEP_{max} values from 2015 to 2022 (Figure 7b, e, h; Table 3). Likewise, daytime mean Tair measured during the CSAD events was far above the $Tair\_NEP_{max}$ threshold for all CSAD events (Figure 7c, f, i; Table 3). In addition, we observed an increase in $Tair\_NEP_{max}$ values from 2015 to 2022 (Figure 7c, f, i; Table 3). Applying the same analysis to daily mean Rff (Figure 8) revealed that daily mean TS measured during the CSAD event in 2018 varied around the TS_Rff_{max} threshold of 2018 (Figure 8a), while measured TS were higher than the TS_Rff_{max} threshold during the CSAD event in 2022 (Figure 8b). As observed for the NEP, SWC values measured during the CSAD events of 2018 and 2022 were far below the respective SWC_Rff_{max} thresholds (Figure 8b, d), with measured data as well as SWC_Rff_{max} thresholds being much lower in 2022 than in 2018 (Figure 8b, d; Table 3).

Table 3. Absolute driver thresholds (mean ± SE) related to the most positive effect on NEP or Rff during the three CSAD years and the long-term means (2005-2022 for NEP and 2019-2021 for Rff). Identification was based on the maximum marginal contribution of the respective driver (VPD, SWC, Tair and TS) in the SHAP analysis for each year.

Year	VPD_NEP_{max} (kPa)	SWC_NEP_{max} (normalised)	$Tair\_NEP_{max}$ (°C)	TS_Rff_{max} (°C)	SWC_Rff_{max} (normalised)
2015	0.66 ± 0.04	0.40 ± 0.43	9.79 ± 0.56	n.a.	n.a.
2018	0.84 ± 0.05	0.14 ± 0.6	13.13 ± 0.30	19.15 ± 0.07	0.58 ± 0.07
2022	0.77 ± 0.06	-0.86 ± 0.4	15.95± 0.37	15.60 ± 0.07	- 0.73 ± 0.09

https://doi.org/10.5194/egusphere-2024-459
Preprint. Discussion started: 26 February 2024

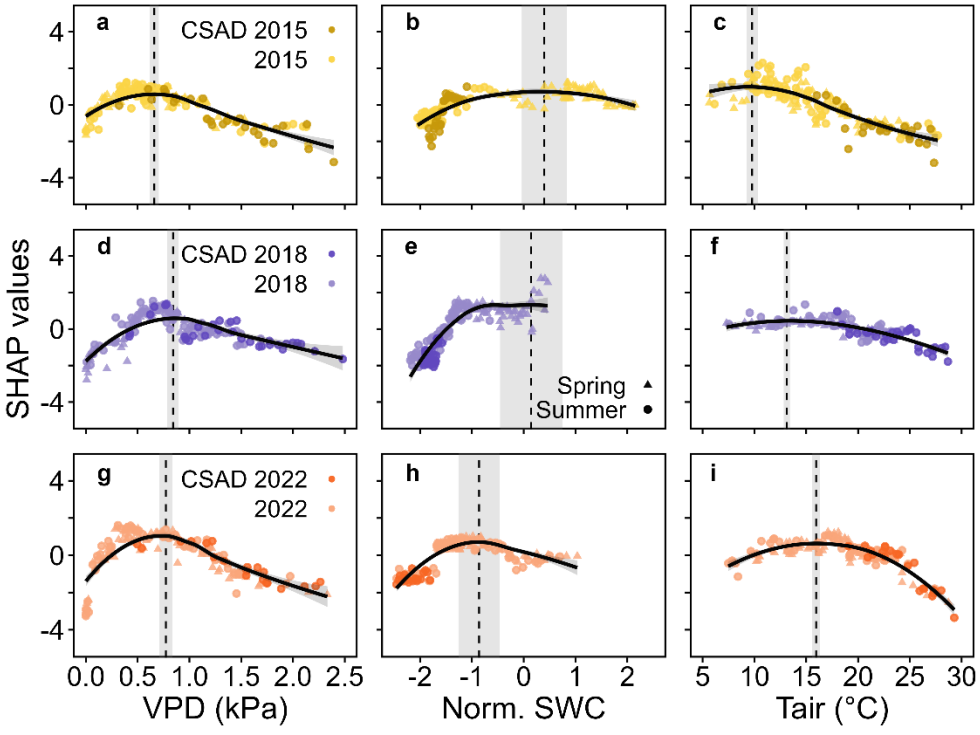

Figure 7. Detection of VPD, SWC and Tair values corresponding to the maximum rate of daytime mean net ecosystem production (NEP) during the growing seasons of 2015, 2018 and 2022. Positive or negative SHAP values represent positive or negative effects on NEP. The vertical dashed lines and the grey ribbons show VPD (a, d, g), SWC (b, e, h), and Tair (c, f, i) and their standard deviations corresponding to the most positive effect on NEP based on the respective maximum marginal contribution of the respective driver in the SHAP analysis for each year to NEP for 2015, 2018 and 2022.

https://doi.org/10.5194/egusphere-2024-459
Preprint. Discussion started: 26 February 2024

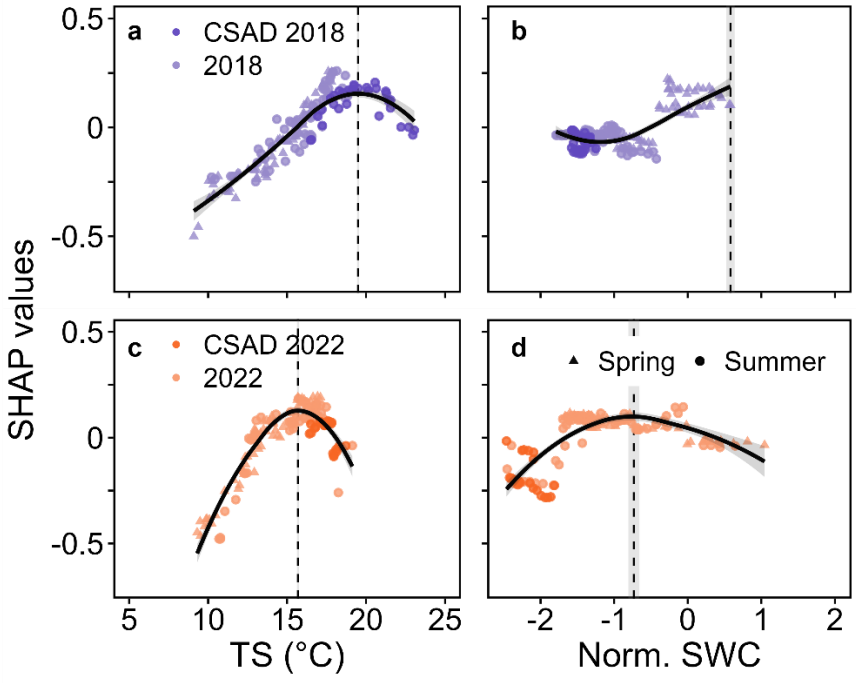

Figure 8. Detection of soil temperature (TS) and SWC values corresponding to the maximum rate of daily mean forest floor respiration (Rff) in 2018 and 2022. Positive or negative SHAP values represent positive or negative effects on Rff. The vertical dashed lines and grey ribbons show TS (a, c) and SWC (b, d) and their standard deviations corresponding to the most positive effect on Rff based on the respective maximum marginal contribution of the respective driver in the SHAP analysis for each year to Rff in 2018 and 2022.

3.4 SR responses to TS and SWC in 2022

As seen above, daily mean SR rates mirrored the responses of Rff (Figure 3), though with a much coarser time resolution. The relationships of SR with TS and SWC varied depending if CSAD events were considered or not (Figure 9). When no CSAD event was recorded, daily mean SR significantly increased with TS (R^2 of 0.76, *P* of 0.002; linear regression). However, during the CSAD event, daily mean SR tended to decrease with increasing TS (Figure 9a). On the other hand, when no CSAD event was recorded, daily mean SR did not respond to variation in SWC ($R^2 < 0.01$), while daily mean SR tended to increase with SWC during the CSAD event (R^2 of 0.3; Figure 9b).

https://doi.org/10.5194/egusphere-2024-459
Preprint. Discussion started: 26 February 2024

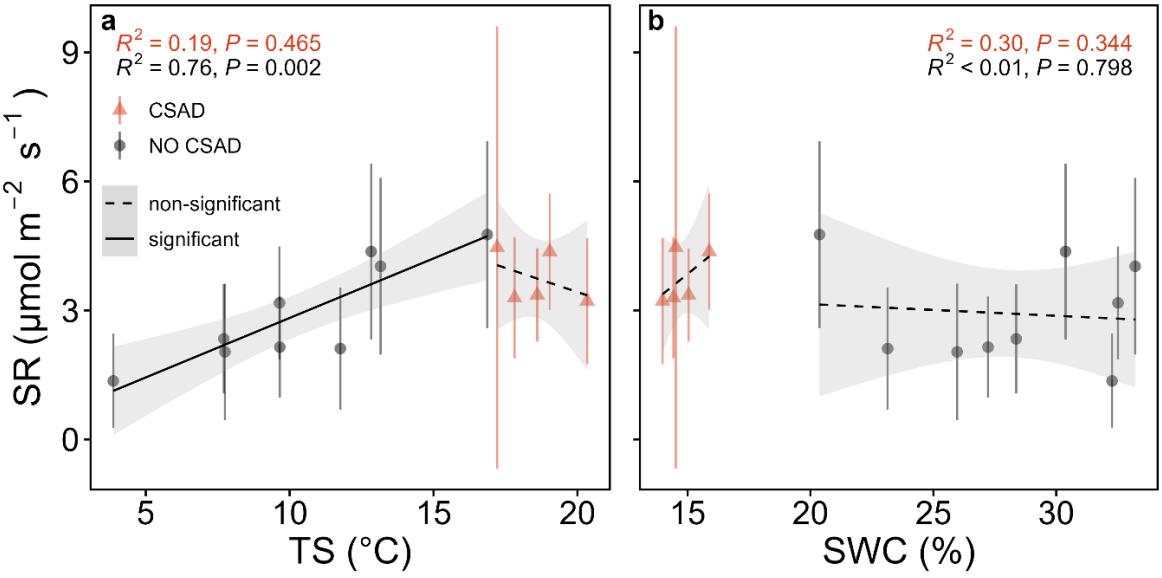

Figure 9. Linear relationships of daily mean soil respiration (SR) with (a) soil temperature (TS) and (b) soil water content (SWC) during the CSAD event 2022 and the rest of the year 2022. Two models were fitted separately for the periods with and without the CSAD event. The goodness of the fit is expressed with R^2 and p-values (P) in the respective panels according to the colour scale.

4 Discussion

In this study, we identified three compound soil and atmospheric drought (CSAD) events during the last 18 years (i.e., 2015, 2018, and 2022) for a mountain mixed deciduous forest. Although they were of comparable intensity, they differed in terms of their timing. We further assessed the mainly negative impacts of these CSAD events on ecosystem CO_2 fluxes (NEP, GPP, Reco) and forest floor respiration (Rff). Moreover, we quantified the temporal contribution of the main drivers to these fluxes during the CSAD events and the respective growing seasons (VPD, Tair, Rg, SWC, TS). Pronounced differences in driver impacts as well as their temporal development were found, for ecosystem vs. forest floor fluxes, but also among drivers and among CSAD events. In addition, we saw first signs of acclimation to such CSAD events, making predictions of site-specific CSADs and their impacts more challenging in the future.

4.1 Compound soil and atmospheric drought (CSAD) events

Several recent studies have shown that Europe already did and also will experience an increase in intensity and frequency of CSAD conditions in the future (e.g., Shekhar et al., 2023; Markonis et al., 2021). Such increased occurrence of extremes was also evident during the 18 years (2005-2022) of eddy-covariance measurements at CH-Lae, with three years (2015, 2018, 2022) being characterized by CSAD events, all within the last eight years (2015-2022). Two other years, 2019 and 2020, also characterized by atmospheric drought, albeit at lower intensity than the three years chosen (Figure 1), did not show co-occurring soil drought at our forest site, and were therefore not identified as CSAD years. This nicely illustrated site-specific

https://doi.org/10.5194/egusphere-2024-459
Preprint. Discussion started: 26 February 2024

environmental conditions playing a relevant role when discussing the impact of extreme compound events at larger spatial scales (Shekhar et al., 2023). Interestingly, even though the intensities of the CSAD events of 2015, 2018 and 2022 were comparable in terms of SWC and VPD values, the pre-conditions and the time of occurrence were different. Pre-conditions (late-spring or early summer), especially in terms of soil moisture and temperature or VPD, can be wet and cool, near-normal, or dry and warm. Thus, depending on these pre-conditions, the impact of any CSAD event on forest performance will differ as shown here. Prior to a CSAD event, soil moisture plays a vital role in determining how well the forest can resist and also recover from the stress of a CSAD event (Jiao et al., 2021). Dry and warm vs. non-limiting conditions before the CSAD event can put the forest under additional water stress during the CSAD event, making it more susceptible to drought and heat stress (da Costa et al., 2018). However, even prior normal soil moisture and warm conditions in spring which favour productivity, but are also accompanied by increased water demands for evapotranspiration, lead to increased soil drying, and can thus amplify extreme dryness stress during summer drought as observed during the 2018 CSAD event at our mixed deciduous forest site (CH-Lae) and across Central Europe (Gharun et al., 2020; Bastos et al., 2020; Shekhar et al., 2020). Thus, CSAD events will require our full attention in the future, since their impacts will strongly differ not only depending on their frequency, duration, and intensity, but also depending on the prior site-specific environmental conditions the ecosystem experiences.

4.2 CO_2 fluxes and their drivers

4.2.1 Net Ecosystem Productivity, NEP

The CSAD events of 2015, 2018 and 2022 resulted in a significant decrease in NEP, which was largely due to decreasing GPP (between 15 and 30%), while ecosystem respiration (Reco) either decreased or did not change compared to the long-term mean at the mixed deciduous forest. Such reductions in GPP during CSAD events have been observed in earlier studies, particularly for beech, the dominant species at our forest site (Ciais et al. 2005; Bastos et al., 2020; Dannenberg et al., 2022; D'Orangeville et al., 2018; Xu et al., 2020; Gharun et al., 2020). Increased stomatal closure in response to high VPD and low soil moisture (i.e., stomatal response), reduction of photosynthesis due to reduced carboxylation rate (Rubisco activity) at high temperatures (i.e., non-stomatal response; Buckley, 2019; Gourlez de la Motte et al., 2020) at leaf level as well as reduced canopy conductance at ecosystem level (Ciais et al. 2003, Granier et al. 2007, Gharun et al. 2020) are typically associated with such CSAD events.

Our driver analysis revealed that air temperature did not have an important impact on reducing NEP during all three CSAD events, suggesting that stomatal responses on GPP were more relevant than temperature-related non-stomatal responses (Granier et al. 2007). Moreover, the major drivers we identified, i.e., VPD and SWC, support stomatal responses as underlying mechanisms for the reduction of net CO_2 uptake via GPP (Dannenberg et al., 2022; Fu et al., 2022; van der Woude et al., 2023) during all three CSAD events in 2015, 2018, and 2022. However, the contributions of those dryness-related variables varied among the CSAD events, suggesting that the response of the forest differed depending on the respective intensity of soil dryness (SWC) and of air dryness (VPD) during the CSAD events. Also, the conditions prior to the CSAD event seemed to

https://doi.org/10.5194/egusphere-2024-459
Preprint. Discussion started: 26 February 2024

play an important role, as SWC was more important for NEP during the 2022 CSAD event, which followed upon a prevailing soil drought, compared to the 2015 and 2018 CSAD events.

Another line of argumentation towards dryness-related vs. temperature-related drivers of reduced NEP during CSAD events is related to Reco with its two major components, i.e., plant and soil respiration. In our study, Reco was between 6-30 % lower during the three CSAD events compared to the other years, supporting the dryness- over the temperature-related argumentation. While plant respiration typically increases in response to high temperatures (Schulze et al. 2019), it also depends on the intensity of the event: if substrate (i.e., carbohydrate) availability is diminished during a CSAD event due to reduced GPP, respiration can also decrease (Janssens et al. 2001; Ciais et al., 2005; Von Buttlar et al., 2018), albeit typically less than GPP (Schwalm et al. 2010). Similarly, soil respiration decreases when substrate supply for root and microbial respiration is low (Högberg et al. 2001; Ruehr et al. 2009). Moreover, soil respiration is known to be small when soil moisture is low (due to reduced microbial and root respiration) during CSAD events (Ruehr et al. 2010; Von Buttlar et al., 2018; Wang et al., 2014), as seen at our site in 2022.

In addition to the standard response of NEP (and its components GPP and Reco) to abiotic factors (VPD, SWC and Tair), NEP sensitivity to abiotic factors could change from one growing season to another, especially during drought conditions, indicating drought acclimation of NEP (Crous et al., 2022; Aspinwall et al., 2017: Sendall et al., 2015; Sperlich et al., 2019). This difference in NEP sensitivity to VPD, SWC and Tair during 2015, 2018, and 2022 growing season was clearly observed in our study (see response curves in Figure 7). The thresholds derived from the response curves of SHAP values vs. the abiotic factors (Figure 7) indicated drought acclimation of NEP to higher VPD (in 2018 and 2022), and lower SWC (in 2022). Such drought acclimations could be due to biophysical adjustments such as access of soil water from deeper soil layers (Brinkmann et al., 2019), changes in photosynthetic thermal acclimation and changes in stomatal sensitivity to VPD (Aspinwall et al., 2017; Smith and Dukes, 2017; Gessler et al., 2020). Such NEP acclimation to higher VPD and lower SWC will be critical in the future, enabling forests to persist (longer) during CSAD events (Kumarathunge et al., 2019).

4.2.2 Forest floor and soil respiration, Rff and SR

The CSAD event in 2022 resulted in a more pronounced and rapid decrease of Rff than in 2018, leading to smaller CO_2 losses from the forest floor compared to 2018 CSAD and the reference period 2019-2021. We observed a similar seasonal trend of Rff and SR, but SR was consistently higher than Rff (Figure 3d). Rff is indeed composed by soil and understory vegetation respiration. At the CH-Lae site, the understory LAI (Leaf Area Index) decreased in late spring (Paul-Limoges, 2017) when trees leaf-out and light reaching the forest floor diminishes. Thus, during the growing season, most of the respiratory CO_2 fluxes from below the canopy consist of SR. Yet, a small part of the SR can be offset by photosynthesis of the vegetation still growing below the canopy (i.e., seedlings of *Fagus sylvatica* and other herbaceous plants). As we observed that GPPff was not different from zero during the growing seasons (Figure A4, appendix A), we here assumed the effect of photosynthesis in the daily Rff being negligible. European mixed forests are usually more resistant to drought than monospecific ones in terms of microbial soil respiration (Gillespie et al., 2020). For example, Gillespie et al. (2020) found that CO_2 emissions were not

https://doi.org/10.5194/egusphere-2024-459
Preprint. Discussion started: 26 February 2024

decreasing under drought in natural mixed European forests. However, a reduction of SR during drought has been widely reported in other studies (e.g., Ruehr et al., 2010; Schindlbacher et al., 2012; Wang et al., 2014; Sun et al., 2019), but the interplay of intensity, duration, and biotic components can trigger different responses of the forest floor in the respective ecosystems (Talmon et al., 2011; Jiao et al., 2021). The decreased importance of TS during the CSAD event of 2018 and 2022 compared to the reference period 2019-2021 (Figure 6) was driven by the limitation of Rff and SR by SWC. In accordance with the SR analysis, we found no effect of TS during the CSAD event in 2022 (Figure 9). Drought periods in forests can indeed diminish the temperature sensitivity of the SR (Jassal et al., 2008; Ruehr et al. 2010; Sun et al., 2019; Schindlbacher et al., 2012; van Straaten et al., 2011; Wang et al., 2014). Generally, SWC is not limiting at the CH-Lae site, but exceptions can occur during summer (Knhol et al., 2008; Ruehr et al., 2010; Trabucco and Zomer, 2022). We know that SR is the sum of heterotrophic and autotrophic respiration (Ruehr and Buchmann, 2009; Wang et al., 2014; Zheng et al., 2021). A large component of heterotrophic respiration is microbial activity in the soil. Under drought, the microbial activity is typically reduced by the limited diffusion of soluble carbon substrate for extracellular enzymes (Manzoni et al., 2012). Consequently, litter decomposition rates also decrease (Deng et al., 2021). If decomposition rates decrease, soil organic matter increases in the soil, resulting in higher C and N in the soil (van der Molen et al., 2011). At the same time, drought reduces photosynthesis and so plants tend to keep non-structural carbohydrates in the leaves to sustain the living tissues (Högberg et al., 2008). Thereby, root activity and production are downregulated (Deng et al., 2021), which can lead to a decoupling of photosynthetic and underground activities (Ruehr et al., 2009; Barba et al., 2018). Eventually, soil drought can significantly alter the N and C cycle in the ecosystem (Deng et al., 2021). The TS and SWC at which Rff_{max} was observed varied from growing season to growing season, as we saw for 2018 and 2022 (Figure 8). The SWC recorded during the CSAD events was clearly below than the SWC_Rff_{max}, but the TS recorded during the CSAD events was observed to be in the range of TS_Rff_{max} in 2018. The interplay and the seasonal trends of TS and SWC can thus determine at which abiotic conditions the highest respiration rate is found. Even though SR is projected to increase under global warming (Schindlbacher et al., 2012), the more frequent occurrence of droughts (Grillakis, 2019) could partially offset those emissions (Zheng et al., 2021), as we observed in the decrease of Rff during CSAD events. However, the decrease in CO_2 emissions can be compensated by CO_2 bursts from rain events occurring after drought periods (Lee et al., 2002) as we observed in after the CSAD event in 2022 (Figure 3d). In general, a recovery of SR is expected if the soil moisture quickly returns to normal conditions (Yao et al., 2023). Yet, biotic factors like fine roots are crucial for trees recovery after drought (Netzer et al., 2016; Hikino et al., 2021; Hikino et al., 2022). For example, it is well known that the fine roots of *Fagus sylvatica* can grow to deeper soil depths during drought, but only if the drought is not too severe, then they can be shed (Hildebrandt, et al., 2020). Indeed, Nickel et al., (2017) found a progressive decrease in vital fine roots after repeated drought in a mixed deciduous forest in Europe. Hence, the pre-and post-conditions, the timing, the intensity, and the duration of a CSAD are very important to predict the consequences in terms of respiratory CO_2 emissions (Wang et al., 2014).

https://doi.org/10.5194/egusphere-2024-459
Preprint. Discussion started: 26 February 2024

5 Conclusions

In this study, we found first signs of forest's NEP to acclimate to more extreme soil (low SWC) and atmospheric drought (high VPD) conditions, which will be fundamental for drought resistance in the future. Nevertheless, we expect to witness a larger reduction of GPP with more extreme CSAD events in the future, even if complemented by a reduction in Reco. Hence responses to CSAD events might lead to a reduction of the CO_2 sink capacity of the forest in the future. The study also highlighted a decoupling between the drivers and the responses of the above canopy and the forest floor CO_2 fluxes during CSAD events. With further global warming in Europe, we expect an increase in Rff, but with more extreme droughts and more intense precipitation events, we assume a higher variability of the CO_2 emissions from forest soils and thus uncertain consequences for the respective soil carbon stocks. Ultimately, the consequences of such events will influence the annual carbon budget of a forest, and thus jeopardising many restoration/reforestation projects or nature-based solutions as proposed in the Paris Agreement.

Appendix A

Table A1. List of instruments, models and manufacturers used in this study.

Instrument	Model	Manufacturer
Infrared gas analyser (IRGA)[1]	LI-7500 (2004-2015)	LI-COR Inc., Lincoln, NE, USA
Infrared gas analyser (IRGA)[1]	LI-7200 (2016-2022)	LI-COR Inc., Lincoln, NE, USA
3-D Sonic anemometer[1]	HS-50	Gill Instruments Ltd., Lymington, UK
Air temperature and relative humidity[2]	Rotronic MP 101 A	Rotronic AG, Bassersdorf, Switzerland
Incoming radiation[2]	BF2_BF2116	Delta-T Devices Ltd, Cambridge, UK
Infrared gas analyser (IRGA)[3]	LI-7500	LI-COR Inc., Lincoln, NE, USA
3-D Sonic anemometer[3]	R-350	Gill Instruments Ltd., Lymington, UK
Air temperature and relative humidiy[4]	CS215_E16511	Campbell Scientific Ltd., UG, USA
Soil temperature and water content[5]	Decagon ECH2O EC-20 probes (2004-2020)	Pullman, WA, USA
Soil temperature and water content[5]	TEROS 12_00007171 (2020-2022)	METER Group AG, NE, USA

https://doi.org/10.5194/egusphere-2024-459
Preprint. Discussion started: 26 February 2024

Incoming radiation[4]	LI190SB-L	LI-COR Inc., Lincoln, NE, USA
Infrared gas analyser (IRGA)[6]	LI-8100	LI-COR Inc., Lincoln, NE, USA
Soil temperature[6]	GTH 175 PT	GHM Messtechnik GmbH, Regenstauf, Germany
Soil water content[6]	HH2 Moisture Meter	Delta-T Devices, Cambridge, United Kingdom

[1]Above-canopy EC system (47 m height)

[2]Above-canopy meteorological measurements (54 m height)

[3]Below-canopy EC system (1.5 m height)

[4]Below-canopy meteorological station (2 m height)

[5]Forest floor meteorological station (profile measurements up to 50 cm depth)

[6]Portable sensors (SR survey measurements)

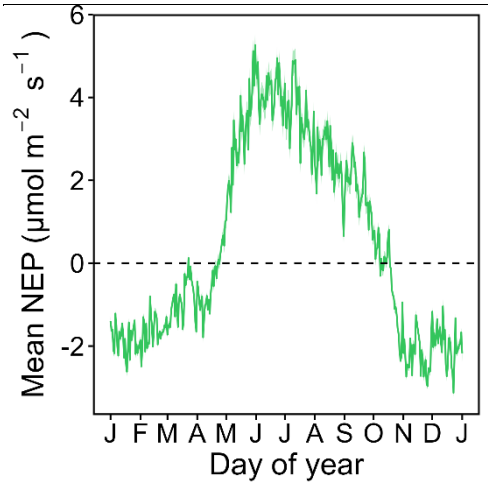

Figure A1. Long-term (2005-2022) daily mean and standard deviation of net ecosystem productivity (NEP) of CH-Lae. The zero-line highlights whether the daily NEP is positive or negative. The growing season (GS) was identified as the period in which daily NEP was positive (1st May to 31st September).

https://doi.org/10.5194/egusphere-2024-459
Preprint. Discussion started: 26 February 2024

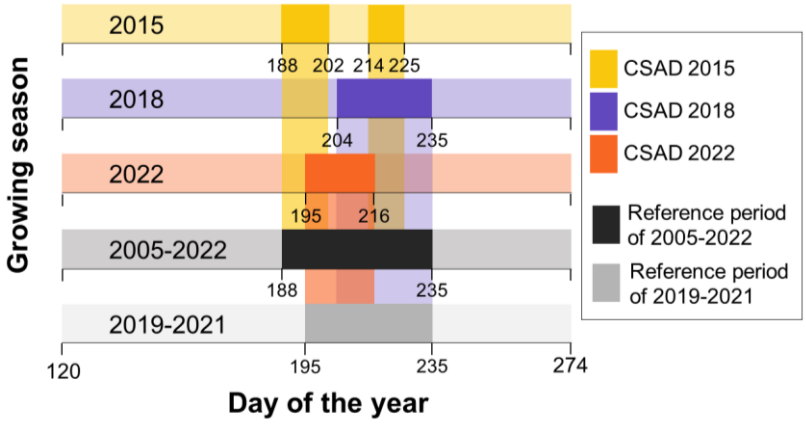

Figure A2. Graphical definition of reference periods. The five horizontal bends display the three growing seasons in which a CSAD event occurred, and the two long term means used as a comparison period (2005-2022 for ecosystem level measurements and 2019-2021 for forest floor measurements). The CSAD periods are marked for each growing season in the CSAD years. The reference period of the mean 2005-2022 used in the analysis corresponds to the interval of time between day 188 (7th July) and day 235 (23rd of August), while the one of the mean 2019-2021 corresponds to the interval of time between day 195 (14th July) and day 235 (23rd of August).

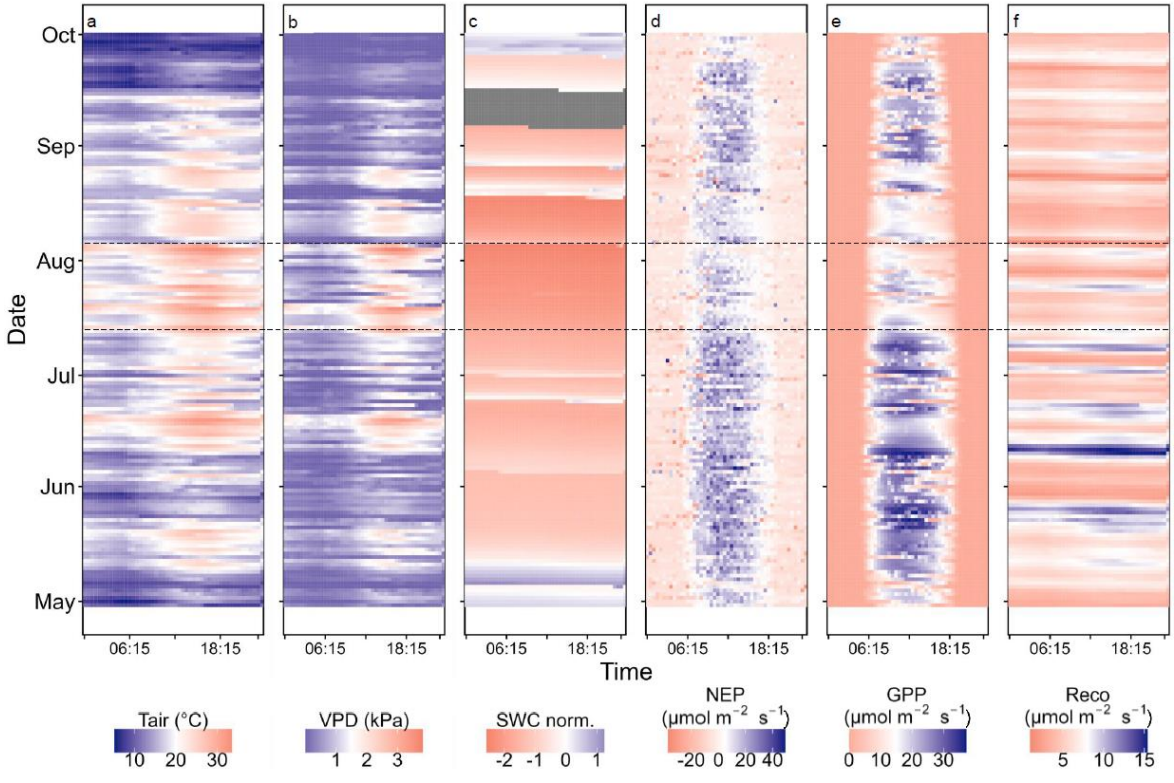

Figure A3. Diurnal (x-axis) and intra-annual (y-axis) variation of (a) air temperature (Tair), (b) VPD, (c) soil water content (SWC at 20 cm depth) (d) net ecosystem production (NEP), (e) gross primary productivity (GPP), and (f) ecosystem respiration (Reco) in

https://doi.org/10.5194/egusphere-2024-459
Preprint. Discussion started: 26 February 2024

2022 growing season. 30 min averages are plotted in all panels. The two black dashed lines extending from 14th July 2022 to 4th August 2022 mark the compound soil and atmospheric drought (CSAD) event of summer 2022.

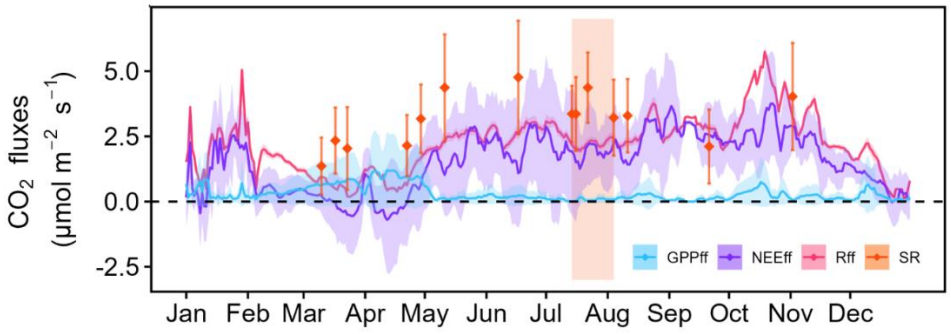

Figure A4. Forest floor CO_2 fluxes in 2022. The continuous lines show gap-filled and partitioned daily mean fluxes and standard deviations (coloured ribbons) of the forest floor. 30 min averages are plotted. The diamonds represent daily means of manual soil respiration measurements, standard deviations are given as well. The orange bend represents the CSAD event of 2022.

Code availability

The R scripts used for the data analysis and plots are available.

Author contribution

LS, AS, MG, NB conceptualization of the study, LS, AS, SAB, AB field campaigns, LS, AS, LH data processing and management, LS, AS data analyses and manuscript writing, and all the authors revision and editing of the manuscript.

Competing interests

The contact author has declared that none of the authors has any competing interests.

Acknowledgements

Authors acknowledge funding from the ETH Zürich project FEVER (ETH-27 19-1), and the SNF funded projects COCO (200021_197357), ICOS-CH Phase 3 (20F120_198227), and EcoDrive (IZCOZ0_198094), and the great support of the Grassland Sciences group members, especially Anna Katarina Gilgen, Luana Krebs, Julia Hauri, Franziska Richter, Yi Wang, Fabio Turco, Ruikun Gou, Roland Anton Werner, and Davide Andreatta.

https://doi.org/10.5194/egusphere-2024-459
Preprint. Discussion started: 26 February 2024

References

Anderegg, W. R. L., Wu, C., Acil, N., Carvalhais, N., Pugh, T. A. M., Sadler, J. P., and Seidl, R.: A climate risk analysis of Earth's forests in the 21st century, Science, 377, 1099-1103, 10.1126/science.abp 9723, 2022.

Aspinwall, M. J., Vårhammar, A., Blackman, C. J., Tjoelker, M. G., Ahrens, C., Byrne, M., Tissue, D. T., and Rymer, P. D.: Adaptation and acclimation both influence photosynthetic and respiratory temperature responses in, Tree Physiology, 37, 1095-1112, 10.1093/treephys/tpx047, 2017.

Aubinet, M., Vesala, T., and Papale, D.: Eddy covariance: a practical guide to measurement and data analysis, Springer Science & Business Media2012.

Barba, J., Lloret, F., Poyatos, R., Molowny-Horas, R., and Yuste, J. C.: Multi-temporal influence of vegetation on soil respiration in a drought-affected forest, Iforest-Biogeosciences and Forestry, 11, 189-198, 10.3832/ifor2448-011, 2018.

Bastos, A., Ciais, P., Friedlingstein, P., Sitch, S., Pongratz, J., Fan, L., Wigneron, J. P., Weber, U., Reichstein, M., Fu, Z., Anthoni, P., Arneth, A., Haverd, V., Jain, A. K., Joetzjer, E., Knauer, J., Lienert, S., Loughran, T., McGuire, P. C., Tian, H., Viovy, N., and Zaehle, S.: Direct and seasonal legacy effects of the 2018 heat wave and drought on European ecosystem productivity, Science Advances, 6, ARTN eaba2724, 10.1126/sciadv.aba2724, 2020.

Bates, D., Mächler, M., Bolker, B. M., and Walker, S. C.: Fitting Linear Mixed-Effects Models Using lme4, Journal of Statistical Software, 67, 1-48, DOI 10.18637/jss.v067.i01, 2015.

Birami, B., Gattmann, M., Heyer, A. G., Grote, R., Arneth, A., and Ruehr, N. K.: Heat Waves Alter Carbon Allocation and Increase Mortality of Aleppo Pine Under Dry Conditions, Frontiers in Forests and Global Change, 1, ARTN 8, 10.3389/ffgc.2018.00008, 2018.

Bogati, K. and Walczak, M.: The Impact of Drought Stress on Soil Microbial Community, Enzyme Activities and Plants, Agronomy-Basel, 12, ARTN 189, 10.3390/agronomy12010189, 2022.

Breiman, L.: Random forests, Machine Learning, 45, 5-32, Doi 10.1023/A:1010933404324, 2001.

Brinkmann, N., Eugster, W., Buchmann, N., and Kahmen, A.: Species-specific differences in water uptake depth of mature temperate trees vary with water availability in the soil, Plant Biology, 21, 71-81, 10.1111/plb.12907, 2019.

Buckley, T. N.: How do stomata respond to water status?, New Phytologist, 224, 21-36, 10.1111/nph.15899, 2019.

Chen, T. and Guestrin, C.: XGBoost: A Scalable Tree Boosting System, Proceedings of the 22nd ACM SIGKDD International Conference on Knowledge Discovery and Data Mining, San Francisco, California, USA, 10.1145/2939672.2939785, 2016.

Chi, J. S., Zhao, P., Klosterhalfen, A., Jocher, G., Kljun, N., Nilsson, M. B., and Peichl, M.: Forest floor fluxes drive differences in the carbon balance of contrasting boreal forest stands, Agricultural and Forest Meteorology, 306, ARTN 108454, 10.1016/j.agrformet.2021.108454, 2021.

Ciais, P., Reichstein, M., Viovy, N., Granier, A., Ogée, J., Allard, V., Aubinet, M., Buchmann, N., Bernhofer, C., Carrara, A., Chevallier, F., De Noblet, N., Friend, A. D., Friedlingstein, P., Grünwald, T., Heinesch, B., Keronen, P., Knohl, A., Krinner, G., Loustau, D., Manca, G., Matteucci, G., Miglietta, F., Ourcival, J. M., Papale, D., Pilegaard, K., Rambal, S., Seufert, G.,

https://doi.org/10.5194/egusphere-2024-459
Preprint. Discussion started: 26 February 2024

Soussana, J. F., Sanz, M. J., Schulze, E. D., Vesala, T., and Valentini, R.: Europe-wide reduction in primary productivity caused by the heat and drought in 2003, Nature, 437, 529-533, 10.1038/nature03972, 2005.

Copernicus Climate Change Service: European State of the Climate 2019, 2019.

Copernicus Climate Change Service (C3S): European State of the Climate 2022, 2023.

Crous, K. Y., Uddling, J., and De Kauwe, M. G.: Temperature responses of photosynthesis and respiration in evergreen trees from boreal to tropical latitudes, New Phytologist, 234, 353-374, 10.1111/nph.17951, 2022.

da Costa, A. C. L., Rowland, L., Oliveira, R. S., Oliveira, A. A. R., Binks, O. J., Salmon, Y., Vasconcelos, S. S., Junior, J. A. S., Ferreira, L. V., Poyatos, R., Mencuccini, M., and Meir, P.: Stand dynamics modulate water cycling and mortality risk in droughted tropical forest, Global Change Biology, 24, 249-258, 10.1111/gcb.13851, 2018.

Dannenberg, M. P., Yan, D., Barnes, M. L., Smith, W. K., Johnston, M. R., Scott, R. L., Biederman, J. A., Knowles, J. F., Wang, X., Duman, T., Litvak, M. E., Kimball, J. S., Williams, A. P., and Zhang, Y.: Exceptional heat and atmospheric dryness amplified losses of primary production during the 2020 U.S. Southwest hot drought, Glob Chang Biol, 28, 4794-4806, 10.1111/gcb.16214, 2022.

de la Motte, L. G., Beauclaire, Q., Heinesch, B., Cuntz, M., Foltynová, L., Sigut, L., Kowalska, N., Manca, G., Ballarin, I. G., Vincke, C., Roland, M., Ibrom, A., Lousteau, D., Siebicke, L., Neiryink, J., and Longdoz, B.: Non-stomatal processes reduce gross primary productivity in temperate forest ecosystems during severe edaphic drought, Philosophical Transactions of the Royal Society B-Biological Sciences, 375, ARTN 20190527, 10.1098/rstb.2019.0527, 2020.

Deng, L., Peng, C. H., Kim, D. G., Li, J. W., Liu, Y. L., Hai, X. Y., Liu, Q. Y., Huang, C. B., Shangguan, Z. P., and Kuzyakov, Y.: Drought effects on soil carbon and nitrogen dynamics in global natural ecosystems, Earth-Science Reviews, 214, ARTN 10350, 10.1016/j.earscirev.2020.103501, 2021.

Dirmeyer, P. A., Balsamo, G., Blyth, E. M., Morrison, R., and Cooper, H. M.: Land-Atmosphere Interactions Exacerbated the Drought and Heatwave Over Northern Europe During Summer 2018, Agu Advances, 2, ARTN e2020AV000283, 10.1029/2020AV000283, 2021.

D'Orangeville, L., Maxwell, J., Kneeshaw, D., Pederson, N., Duchesne, L., Logan, T., Houle, D., Arseneault, D., Beier, C. M., Bishop, D. A., Druckenbrod, D., Fraver, S., Girard, F., Halman, J., Hansen, C., Hart, J. L., Hartmann, H., Kaye, M., Leblanc, D., Manzoni, S., Ouimet, R., Rayback, S., Rollinson, C. R., and Phillips, R. P.: Drought timing and local climate determine the sensitivity of eastern temperate forests to drought, Global Change Biology, 24, 2339-2351, 10.1111/gcb.14096, 2018.

Etzold, S., Buchmann, N., and Eugster, W.: Contribution of advection to the carbon budget measured by eddy covariance at a steep mountain slope forest in Switzerland, Biogeosciences, 7, 2461-2475, 10.5194/bg-7-2461-2010, 2010.

Etzold, S., Ruehr, N. K., Zweifel, R., Dobbertin, M., Zingg, A., Pluess, P., Häsler, R., Eugster, W., and Buchmann, N.: The Carbon Balance of Two Contrasting Mountain Forest Ecosystems in Switzerland: Similar Annual Trends, but Seasonal Differences, Ecosystems, 14, 1289-1309, 10.1007/s10021-011-9481-3, 2011.

https://doi.org/10.5194/egusphere-2024-459
Preprint. Discussion started: 26 February 2024

Fan, S. M., Wofsy, S. C., Bakwin, P. S., Jacob, D. J., and Fitzjarrald, D. R.: Atmosphere-Biosphere Exchange of Co2 and O3 in the Central-Amazon-Forest, Journal of Geophysical Research-Atmospheres, 95, 16851-16864, DOI 10.1029/JD095iD10p16851, 1990.

Foken, T., Göockede, M., Mauder, M., Mahrt, L., Amiro, B., and Munger, W.: Post-field data quality control, in: Handbook of micrometeorology: a guide for surface flux measurement and analysis, Springer, 181-208, 2004.

Fratini, G., Ibrom, A., Arriga, N., Burba, G., and Papale, D.: Relative humidity effects on water vapour fluxes measured with closed-path eddy-covariance systems with short sampling lines (vol 165, pg 53, 2012), Agricultural and Forest Meteorology, 166, 234-234, 10.1016/j.agrformet.2012.10.013, 2012.

Gazol, A. and Camarero, J. J.: Compound climate events increase tree drought mortality across European forests, Science of the Total Environment, 816, ARTN 151604, 10.1016/j.scitotenv.2021.151604, 2022.

George, J. P., Bürkner, P. C., Sanders, T. G. M., Neumann, M., Cammalleri, C., Vogt, J. V., and Lang, M.: Long-term forest monitoring reveals constant mortality rise in European forests, Plant Biology, 24, 1108-1119, 10.1111/plb.13469, 2022.

Gessler, A., Bottero, A., Marshall, J., and Arend, M.: The way back: recovery of trees from drought and its implication for acclimation, New Phytologist, 228, 1704-1709, 10.1111/nph.16703, 2020.

Gharun, M., Hörtnagl, L., Paul-Limoges, E., Ghiasi, S., Feigenwinter, I., Burri, S., Marquardt, K., Etzold, S., Zweifel, R., Eugster, W., and Buchmann, N.: Physiological response of Swiss ecosystems to 2018 drought across plant types and elevation, Philosophical Transactions of the Royal Society B-Biological Sciences, 375, ARTN 20190521, 10.1098/rstb.2019.0521, 2020.

Gillespie, L. M., Fromin, N., Milcu, A., Buatois, B., Pontoizeau, C., and Hättenschwiler, S.: Higher tree diversity increases soil microbial resistance to drought, Communications Biology, 3, ARTN 377
10.1038/s42003-020-1112-0, 2020.

Gillespie, L. M., Fromin, N., Milcu, A., Buatois, B., Pontoizeau, C., and Hättenschwiler, S.: Higher tree diversity increases soil microbial resistance to drought, Communications Biology, 3, ARTN 377
10.1038/s42003-020-1112-0, 2020.

Grillakis, M. G.: Increase in severe and extreme soil moisture droughts for Europe under climate change, Science of the Total Environment, 660, 1245-1255, 10.1016/j.scitotenv.2019.01.001, 2019.

Grossiord, C., Buckley, T. N., Cernusak, L. A., Novick, K. A., Poulter, B., Siegwolf, R. T. W., Sperry, J. S., and McDowell, N. G.: Plant responses to rising vapor pressure deficit, New Phytologist, 226, 1550-1566, 10.1111/nph.16485, 2020.

Grossiord, C., Sevanto, S., Borrego, I., Chan, A. M., Collins, A. D., Dickman, L. T., Hudson, P. J., McBranch, N., Michaletz, S. T., Pockman, W. T., Ryan, M., Vilagrosa, A., and McDowell, N. G.: Tree water dynamics in a drying and warming world, Plant Cell and Environment, 40, 1861-1873, 10.1111/pce.12991, 2017.

Haberstroh, S., Werner, C., Grün, M., Kreuzwieser, J., Seifert, T., Schindler, D., and Christen, A.: Central European 2018 hot drought shifts scots pine forest to its tipping point, Plant Biology, 24, 1186-1197, 10.1111/plb.13455, 2022.

Harris, N. L., Gibbs, D. A., Baccini, A., Birdsey, R. A., de Bruin, S., Farina, M., Fatoyinbo, L., Hansen, M. C., Herold, M., Houghton, R. A., Potapov, P. V., Suarez, D. R., Roman-Cuesta, R. M., Saatchi, S. S., Slay, C. M., Turubanova, S. A., and

https://doi.org/10.5194/egusphere-2024-459
Preprint. Discussion started: 26 February 2024

Tyukavina, A.: Global maps of twenty-first century forest carbon fluxes, Nature Climate Change, 11, 10.1038/s41558-020-00976-6, 2021.

Hermann, M., Röthlisberger, M., Gessler, A., Rigling, A., Senf, C., Wohlgemuth, T., and Wernli, H.: Meteorological history of low-forest-greenness events in Europe in 2002-2022, Biogeosciences, 20, 1155-1180, 10.5194/bg-20-1155-2023, 2023.

Hikino, K., Danzberger, J., Riedel, V. P., Rehschuh, R., Ruehr, N. K., Hesse, B. D., Lehmann, M. M., Buegger, F., Weikl, F., Pritsch, K., and Grams, T. E. E.: High resilience of carbon transport in long-term drought-stressed mature Norway spruce trees within 2 weeks after drought release, Global Change Biology, 28, 2095-2110, 10.1111/gcb.16051, 2022.

Hikino, K., Danzberger, J., Riedel, V. P., Hesse, B. D., Hafner, B. D., Gebhardt, T., Rehschuh, R., Ruehr, N. K., Brunn, M., Bauerle, T. L., Landhäusser, S. M., Lehmann, M. M., Rötzer, T., Pretzsch, H., Buegger, F., Weikl, F., Pritsch, K., and Grams, T. E. E.: Dynamics of initial carbon allocation after drought release in mature Norway spruce-Increased belowground allocation of current photoassimilates covers only half of the carbon used for fine-root growth, Global Change Biology, 28, 6889-6905, 10.1111/gcb.16388, 2022.

Hildebrandt, A.: Root-Water Relations and Interactions in Mixed Forest Settings, Forest-Water Interactions, 240, 319-348, 10.1007/978-3-030-26086-6_14, 2020.

Högberg, P., Nordgren, A., Buchmann, N., Taylor, A. F. S., Ekblad, A., Högberg, M. N., Nyberg, G., Ottosson-Löfvenius, M., and Read, D. J.: Large-scale forest girdling shows that current photosynthesis drives soil respiration, Nature, 411, 789-792, Doi 10.1038/35081058, 2001.

Högberg, P., Högberg, M. N., Göttlicher, S. G., Betson, N. R., Keel, S. G., Metcalfe, D. B., Campbell, C., Schindlbacher, A., Hurry, V., Lundmark, T., Linder, S., and Näsholm, T.: High temporal resolution tracing of photosynthate carbon from the tree canopy to forest soil microorganisms, New Phytologist, 177, 220-228, 10.1111/j.1469-8137.2007.02238.x, 2008.

Horst, T. W.: A simple formula for attenuation of eddy fluxes measured with first-order-response scalar sensors, Boundary-Layer Meteorology, 82, 219-233, Doi 10.1023/A:1000229130034, 1997.

Hothorn, T., Hornik, K., and Zeileis, A.: Unbiased recursive partitioning: A conditional inference framework, Journal of Computational and Graphical Statistics, 15, 651-674, 10.1198/106186006x133933, 2006.

Intergovernmental Panel on Climate, C.: Climate Change 2022 – Impacts, Adaptation and Vulnerability: Working Group II Contribution to the Sixth Assessment Report of the Intergovernmental Panel on Climate Change, Cambridge University Press, Cambridge, DOI: 10.1017/9781009325844, 2023.

Ionita, M., Dima, M., Nagavciuc, V., Scholz, P., and Lohmann, G.: Past megadroughts in central Europe were longer, more severe and less warm than modern droughts, Communications Earth & Environment, 2, ARTN 61 10.1038/s43247-021-00130-w, 2021.

Ionita, M., Tallaksen, L. M., Kingston, D. G., Stagge, J. H., Laaha, G., Van Lanen, H. A. J., Scholz, P., Chelcea, S. M., and Haslinger, K.: The European 2015 drought from a climatological perspective, Hydrology and Earth System Sciences, 21, 1397-1419, 10.5194/hess-21-1397-2017, 2017.

https://doi.org/10.5194/egusphere-2024-459
Preprint. Discussion started: 26 February 2024

669 Janssens, I. A., Lankreijer, H., Matteucci, G., Kowalski, A. S., Buchmann, N., Epron, D., Pilegaard, K., Kutsch, W., Longdoz,
670 B., Grünwald, T., Montagnani, L., Dore, S., Rebmann, C., Moors, E. J., Grelle, A., Rannik, Ü., Morgenstern, K., Oltchev, S.,
671 Clement, R., Gudmundsson, J., Minerbi, S., Berbigier, P., Ibrom, A., Moncrieff, J., Aubinet, M., Bernhofer, C., Jensen, N. O.,
672 Vesala, T., Granier, A., Schulze, E. D., Lindroth, A., Dolman, A. J., Jarvis, P. G., Ceulemans, R., and Valentini, R.:
673 Productivity overshadows temperature in determining soil and ecosystem respiration across European forests, Global Change
674 Biology, 7, 269-278, DOI 10.1046/j.1365-2486.2001.00412.x, 2001.
675 Jassal, R. S., Black, T. A., Novak, M. D., Gaumont-Guay, D., and Nesic, Z.: Effect of soil water stress on soil respiration and
676 its temperature sensitivity in an 18-year-old temperate Douglas-fir stand, Global Change Biology, 14, 1305-1318,
677 10.1111/j.1365-2486.2008.01573.x, 2008.
678 Jiao, T., Williams, C. A., De Kauwe, M. G., Schwalm, C. R., and Medlyn, B. E.: Patterns of post-drought recovery are strongly
679 influenced by drought duration, frequency, post-drought wetness, and bioclimatic setting, Global Change Biology, 27, 4630-
680 4643, 10.1111/gcb.15788, 2021.
681 Kim, J. B., So, J. M., and Bae, D. H.: Global Warming Impacts on Severe Drought Characteristics in Asia Monsoon Region,
682 Water, 12, ARTN 1360
683 10.3390/w12051360, 2020.
684 Kittler, F., Eugster, W., Foken, T., Heimann, M., Kolle, O., and Göckede, M.: High-quality eddy-covariance CO
685 budgets under cold climate conditions, Journal of Geophysical Research-Biogeosciences, 122, 2064-2084,
686 10.1002/2017jg003830, 2017.
687 Knohl, A., Soe, A. R. B., Kutsch, W. L., Göckede, M., and Buchmann, N.: Representative estimates of soil and ecosystem
688 respiration in an old beech forest, Plant and Soil, 302, 189-202, 10.1007/s11104-007-9467-2, 2008.
689 Körner, C., Möhl, P., and Hiltbrunner, E.: Four ways to define the growing season, Ecology Letters, 10.1111/ele.14260, 2023.
690 Kumarathunge, D. P., Medlyn, B. E., Drake, J. E., Tjoelker, M. G., Aspinwall, M. J., Battaglia, M., Cano, F. J., Carter, K. R.,
691 Cavaleri, M. A., Cernusak, L. A., Chambers, J. Q., Crous, K. Y., De Kauwe, M. G., Dillaway, D. N., Dreyer, E., Ellsworth, D.
692 S., Ghannoum, O., Han, Q. M., Hikosaka, K., Jensen, A. M., Kelly, J. W. G., Kruger, E. L., Mercado, L. M., Onoda, Y., Reich,
693 P. B., Rogers, A., Slot, M., Smith, N. G., Tarvainen, L., Tissue, D. T., Togashi, H. F., Tribuzy, E. S., Uddling, J., Vårhammar,
694 A., Wallin, G., Warren, J. M., and Way, D. A.: Acclimation and adaptation components of the temperature dependence of
695 plant photosynthesis at the global scale, New Phytologist, 222, 768-784, 10.1111/nph.15668, 2019.
696 Lal, P., Shekhar, A., Gharun, M., and Das, N. N.: Spatiotemporal evolution of global long-term patterns of soil moisture,
697 Science of the Total Environment, 867, ARTN 161470, 10.1016/j.scitotenv.2023.161470, 2023.
698 Lasslop, G., Reichstein, M., Papale, D., Richardson, A. D., Arneth, A., Barr, A., Stoy, P., and Wohlfahrt, G.: Separation of net
699 ecosystem exchange into assimilation and respiration using a light response curve approach: critical issues and global
700 evaluation, Global Change Biology, 16, 187-208, 10.1111/j.1365-2486.2009.02041.x, 2010.
701 Lee, M. S., Nakane, K., Nakatsubo, T., Mo, W. H., and Koizumi, H.: Effects of rainfall events on soil CO_2 flux in a cool
702 temperate deciduous broad-leaved forest, Ecological Research, 17, 401-409, UNSP ere_498.sgm

DOI 10.1046/j.1440-1703.2002.00498.x, 2002.

Lloyd, J. and Taylor, J. A.: On the Temperature-Dependence of Soil Respiration, Functional Ecology, 8, 315-323, Doi 10.2307/2389824, 1994.

Lu, R. Y., Xu, K., Chen, R. D., Chen, W., Li, F., and Lv, C. Y.: Heat waves in summer 2022 and increasing concern regarding heat waves in general, Atmospheric and Oceanic Science Letters, 16, ARTN 100290, 10.1016/j.aosl.2022.100290, 2023.

Lundberg, S. M. and Lee, S. I.: A Unified Approach to Interpreting Model Predictions, Advances in Neural Information Processing Systems 30 (Nips 2017), 30, 2017.

Lundberg, S. M., Erion, G., Chen, H., DeGrave, A., Prutkin, J. M., Nair, B., Katz, R., Himmelfarb, J., Bansal, N., and Lee, S. I.: From local explanations to global understanding with explainable AI for trees, Nature Machine Intelligence, 2, 56-67, 10.1038/s42256-019-0138-9, 2020.

Manzoni, S., Schimel, J. P., and Porporato, A.: Responses of soil microbial communities to water stress: results from a meta-analysis, Ecology, 93, 930-938, Doi 10.1890/11-0026.1, 2012.

Markonis, Y., Kumar, R., Hanel, M., Rakovec, O., Máca, P., and AghaKouchak, A.: The rise of compound warm-season droughts in Europe, Science Advances, 7, ARTN eabb9668, 10.1126/sciadv.abb9668, 2021.

Martinez-Garcia, E., Nilsson, M. B., Laudon, H., Lundmark, T., Fransson, J. E. S., Wallerman, J., and Peichl, M.: Overstory dynamics regulate the spatial variability in forest-floor CO2 fluxes across a managed boreal forest landscape, Agricultural and Forest Meteorology, 318, ARTN 108916, 10.1016/j.agrformet.2022.108916, 2022.

MeteoSvizzera. (2023). Rapporto sul clima 2022.

Miralles, D. G., Gentine, P., Seneviratne, S. I., and Teuling, A. J.: Land-atmospheric feedbacks during droughts and heatwaves: state of the science and current challenges, Annals of the New York Academy of Sciences, 1436, 19-35, 10.1111/nyas.13912, 2019.

Moncrieff, J., Clement, R., Finnigan, J., and Meyers, T.: Averaging, detrending, and filtering of eddy covariance time series, in: Handbook of micrometeorology: A guide for surface flux measurement and analysis, Springer, 7-31, 2004.

Moravec, V., Markonis, Y., Rakovec, O., Svoboda, M., Trnka, M., Kumar, R., and Hanel, M.: Europe under multi-year droughts: how severe was the 2014-2018 drought period?, Environmental Research Letters, 16, ARTN 03406210.1088/1748-9326/abe828, 2021.

Netzer, F., Thöm, C., Celepirovic, N., Ivankovic, M., Alfarraj, S., Dounavi, A., Simon, J., Herschbach, C., and Rennenberg, H.: Drought effects on C, N, and P nutrition and the antioxidative system of beech seedlings depend on geographic origin, Journal of Plant Nutrition and Soil Science, 179, 136-150, 10.1002/jpln.201500461, 2016.

Nickel, U. T., Weikl, F., Kerner, R., Schäfer, C., Kallenbach, C., Munch, J. C., and Pritsch, K.: Quantitative losses vs. qualitative stability of ectomycorrhizal community responses to 3 years of experimental summer drought in a beech-spruce forest, Global Change Biology, 24, E560-E576, 10.1111/gcb.13957, 2018.

https://doi.org/10.5194/egusphere-2024-459
Preprint. Discussion started: 26 February 2024

Obladen, N., Dechering, P., Skiadaresis, G., Tegel, W., Kessler, J., Höllerl, S., Kaps, S., Hertel, M., Dulamsuren, C., Seifert, T., Hirsch, M., and Seim, A.: Tree mortality of European beech and Norway spruce induced by 2018-2019 hot droughts in central Germany, Agricultural and Forest Meteorology, 307, ARTN 108482 10.1016/j.agrformet.2021.108482, 2021.

Orth, R.: When the Land Surface Shifts Gears, Agu Advances, 2, ARTN e2021AV000414, 10.1029/2021AV000414, 2021.

Paul-Limoges, E., Wolf, S., Eugster, W., Hörtnagl, L., and Buchmann, N.: Below-canopy contributions to ecosystem CO_2 fluxes in a temperate mixed forest in Switzerland, Agricultural and Forest Meteorology, 247, 582-596, 10.1016/j.agrformet.2017.08.011, 2017.

Paul-Limoges, E., Wolf, S., Schneider, F. D., Longo, M., Moorcroft, P., Gharun, M., and Damm, A.: Partitioning evapotranspiration with concurrent eddy covariance measurements in a mixed forest, Agricultural and Forest Meteorology, 280, ARTN 10778610.1016/j.agrformet.2019.107786, 2020.

Pei, F. S., Li, X., Liu, X. P., and Lao, C. H.: Assessing the impacts of droughts on net primary productivity in China, Journal of Environmental Management, 114, 362-371, 10.1016/j.jenvman.2012.10.031, 2013.

Reichstein, M., Falge, E., Baldocchi, D., Papale, D., Aubinet, M., Berbigier, P., Bernhofer, C., Buchmann, N., Gilmanov, T., Granier, A., Grünwald, T., Havránková, K., Ilvesniemi, H., Janous, D., Knohl, A., Laurila, T., Lohila, A., Loustau, D., Matteucci, G., Meyers, T., Miglietta, F., Ourcival, J. M., Pumpanen, J., Rambal, S., Rotenberg, E., Sanz, M., Tenhunen, J., Seufert, G., Vaccari, F., Vesala, T., Yakir, D., and Valentini, R.: On the separation of net ecosystem exchange into assimilation and ecosystem respiration:: review and improved algorithm, Global Change Biology, 11, 1424-1439, 10.1111/j.1365-2486.2005.001002.x, 2005.

Ruehr, N. K. and Buchmann, N.: Soil respiration fluxes in a temperate mixed forest: seasonality and temperature sensitivities differ among microbial and root-rhizosphere respiration, Tree Physiology, 30, 165-176, 10.1093/treephys/tpp106, 2010.

Ruehr, N. K., Knohl, A., and Buchmann, N.: Environmental variables controlling soil respiration on diurnal, seasonal and annual time-scales in a mixed mountain forest in Switzerland, Biogeochemistry, 98, 153-170, 10.1007/s10533-009-9383-z, 2010.

Ruehr, N. K., Offermann, C. A., Gessler, A., Winkler, J. B., Ferrio, J. P., Buchmann, N., and Barnard, R. L.: Drought effects on allocation of recent carbon: from beech leaves to soil CO_2 efflux, New Phytologist, 184, 950-961, 10.1111/j.1469-8137.2009.03044.x, 2009.

Rukh, S., Sanders, T. G. M., Krüger, I., Schad, T., and Bolte, A.: Distinct Responses of European Beech (L.) to Drought Intensity and Length-A Review of the Impacts of the 2003 and 2018-2019 Drought Events in Central Europe, Forests, 14, ARTN 24810.3390/f14020248, 2023.

Sabbatini, S., Mammarella, I., Arriga, N., Fratini, G., Graf, A., Hörtriagl, L., Ibrom, A., Longdoz, B., Mauder, M., Merbold, L., Metzger, S., Montagnani, L., Pitacco, A., Rebmann, C., Sedlák, P., Sigut, L., Vitale, D., and Papale, D.: Eddy covariance raw data processing for CO_2 and energy fluxes calculation at ICOS ecosystem stations, International Agrophysics, 32, 495-+, 10.1515/intag-2017-0043, 2018.

https://doi.org/10.5194/egusphere-2024-459
Preprint. Discussion started: 26 February 2024

769 Schindlbacher, A., Wunderlich, S., Borken, W., Kitzler, B., Zechmeister-Boltenstern, S., and Jandl, R.: Soil respiration under
770 climate change: prolonged summer drought offsets soil warming effects, Global Change Biology, 18, 2270-2279,
771 10.1111/j.1365-2486.2012.02696.x, 2012.
772 Schuldt, B., Buras, A., Arend, M., Vitasse, Y., Beierkuhnlein, C., Damm, A., Gharun, M., Grams, T. E. E., Hauck, M., Hajek,
773 P., Hartmann, H., Hiltbrunner, E., Hoch, G., Holloway-Phillips, M., Körner, C., Larysch, E., Lübbe, T., Nelson, D. B.,
774 Rammig, A., Rigling, A., Rose, L., Ruehr, N. K., Schumann, K., Weiser, F., Werner, C., Wohlgemuth, T., Zang, C. S., and
775 Kahmen, A.: A first assessment of the impact of the extreme 2018 summer drought on Central European forests, Basic and
776 Applied Ecology, 45, 86-103, 10.1016/j.baae.2020.04.003, 2020.
777 Schulze ED, B. E., Buchmann N, Clemens S, Müller-Hohenstein K, Scherer-Lorenzen M Springer (Ed.): Plant Ecology, 2,
778 928 pp.2019.
779 Schwalm, C. R., Williams, C. A., Schaefer, K., Arneth, A., Bonal, D., Buchmann, N., Chen, J. Q., Law, B. E., Lindroth, A.,
780 Luyssaert, S., Reichstein, M., and Richardson, A. D.: Assimilation exceeds respiration sensitivity to drought: A FLUXNET
781 synthesis, Global Change Biology, 16, 657-670, 10.1111/j.1365-2486.2009.01991.x, 2010.
782 Sendall, K. M., Reich, P. B., Zhao, C. M., Hou, J. H., Wei, X. R., Stefanski, A., Rice, K., Rich, R. L., and Montgomery, R. A.:
783 Acclimation of photosynthetic temperature optima of temperate and boreal tree species in response to experimental forest
784 warming, Global Change Biology, 21, 1342-1357, 10.1111/gcb.12781, 2015.
785 Shekhar, A., Humphrey, V., Buchmann, N., and Gharun, M.: More than three-fold increase of extreme dryness across Europe
786 by end of 21st century, 10.21203/rs.3.rs-3143908/v2, 2023.
787 Shekhar, A., Chen, J., Bhattacharjee, S., Buras, A., Castro, A. O., Zang, C. S., and Rammig, A.: Capturing the Impact of the
788 2018 European Drought and Heat across Different Vegetation Types Using OCO-2 Solar-Induced Fluorescence, Remote
789 Sensing, 12, ARTN 3249, 10.3390/rs12193249, 2020.
790 Shekhar, A., Hörtnagl, L., Paul-Limoges, E., Etzold, S., Zweifel, R., Buchmann, N., and Gharun, M.: Contrasting impact of
791 extreme soil and atmospheric dryness on the functioning of trees and forests, Science of The Total Environment, 169931,
792 2024.
793 Smith, N. G. and Dukes, J. S.: Short-term acclimation to warmer temperatures accelerates leaf carbon exchange processes
794 across plant types, Global Change Biology, 23, 4840-4853, 10.1111/gcb.13735, 2017.
795 Sperlich, D., Chang, C. T., Peñuelas, J., and Sabaté, S.: Responses of photosynthesis and component processes to drought and
796 temperature stress: are Mediterranean trees fit for climate change?, Tree Physiology, 39, 1783-1805, 10.1093/treephys/tpz089,
797 2019.
798 Spinoni, J., Vogt, J. V., Naumann, G., Barbosa, P., and Dosio, A.: Will drought events become more frequent and severe in
799 Europe?, International Journal of Climatology, 38, 1718-1736, 10.1002/joc.5291, 2018.
800 Sun, S. Q., Lei, H. Q., and Chang, S. X.: Drought differentially affects autotrophic and heterotrophic soil respiration rates and
801 their temperature sensitivity, Biology and Fertility of Soils, 55, 275-283, 10.1007/s00374-019-01347-w, 2019.

https://doi.org/10.5194/egusphere-2024-459
Preprint. Discussion started: 26 February 2024

Talmon, Y., Sternberg, M., and Grünzweig, J. M.: Impact of rainfall manipulations and biotic controls on soil respiration in Mediterranean and desert ecosystems along an aridity gradient, Global Change Biology, 17, 1108-1118, 10.1111/j.1365-2486.2010.02285.x, 2011.

Team, R. C.: R: a language and environment for statistical computing. Vienna: R Foundation for Statistical Computing, (No Title), 2021.

Trabucco, A.: Global aridity index and potential evapotranspiration (ET0) climate database v2, CGIAR Consort Spat Inf, 2019.

Tripathy, K. P. and Mishra, A. K.: How Unusual Is the 2022 European Compound Drought and Heatwave Event?, Geophysical Research Letters, 50, ARTN e2023GL105453, 10.1029/2023GL105453, 2023.

van der Molen, M. K., Dolman, A. J., Ciais, P., Eglin, T., Gobron, N., Law, B. E., Meir, P., Peters, W., Phillips, O. L., Reichstein, M., Chen, T., Dekker, S. C., Doubkova, M., Friedl, M. A., Jung, M., van den Hurk, B. J. J. M., de Jeu, R. A. M., Kruijt, B., Ohta, T., Rebel, K. T., Plummer, S., Seneviratne, S. I., Sitch, S., Teuling, A. J., van der Werf, G. R., and Wang, G.: Drought and ecosystem carbon cycling, Agricultural and Forest Meteorology, 151, 765-773, 10.1016/j.agrformet.2011.01.018, 2011.

van der Woude, A. M., Peters, W., Joetzjer, E., Lafont, S., Koren, G., Ciais, P., Ramonet, M., Xu, Y. D., Bastos, A., Botia, S., Sitch, S., de Kok, R., Kneuer, T., Kubistin, D., Jacotot, A., Loubet, B., Herig-Coimbra, P. H., Loustau, D., and Luijkx, I. T.: Temperature extremes of 2022 reduced carbon uptake by forests in Europe, Nature Communications, 14, ARTN 6218, 10.1038/s41467-023-41851-0, 2023.

van Straaten, O., Veldkamp, E., and Corre, M. D.: Simulated drought reduces soil CO_2 efflux and production in a tropical forest in Sulawesi, Indonesia, Ecosphere, 2, Artn 119, 10.1890/Es11-00079.1, 2011.

von Buttlar, J., Zscheischler, J., Rammig, A., Sippel, S., Reichstein, M., Knohl, A., Jung, M., Menzer, O., Arain, M. A., Buchmann, N., Cescatti, A., Gianelle, D., Kiely, G., Law, B. E., Magliulo, V., Margolis, H., McCaughey, H., Merbold, L., Migliavacca, M., Montagnani, L., Oechel, W., Pavelka, M., Peichl, M., Rambal, S., Raschi, A., Scott, R. L., Vaccari, F. P., van Gorsel, E., Varlagin, A., Wohlfahrt, G., and Mahecha, M. D.: Impacts of droughts and extreme-temperature events on gross primary production and ecosystem respiration: a systematic assessment across ecosystems and climate zones, Biogeosciences, 15, 1293-1318, 10.5194/bg-15-1293-2018, 2018.

Wang, Y. F., Hao, Y. B., Cui, X. Y., Zhao, H. T., Xu, C. Y., Zhou, X. Q., and Xu, Z. H.: Responses of soil respiration and its components to drought stress, Journal of Soils and Sediments, 14, 99-109, 10.1007/s11368-013-0799-7, 2014.

Wang, H., Yan, S. J., Ciais, P., Wigneron, J. P., Liu, L. B., Li, Y., Fu, Z., Ma, H. L., Liang, Z., Wei, F. L., Wang, Y. Y., and Li, S. C.: Exploring complex water stress-gross primary production relationships: Impact of climatic drivers, main effects, and interactive effects, Global Change Biology, 28, 4110-4123, 10.1111/gcb.16201, 2022.
Wang, H., Yan, S. J., Ciais, P., Wigneron, J. P., Liu, L. B., Li, Y., Fu, Z., Ma, H. L., Liang, Z., Wei, F. L., Wang, Y. Y., and Li, S. C.: Exploring complex water stress-gross primary production relationships: Impact of climatic drivers, main effects, and interactive effects, Global Change Biology, 28, 4110-4123, 10.1111/gcb.16201, 2022.

https://doi.org/10.5194/egusphere-2024-459
Preprint. Discussion started: 26 February 2024

Webb, E. K., Pearman, G. I., and Leuning, R.: Correction of Flux Measurements for Density Effects Due to Heat and Water-Vapor Transfer, Quarterly Journal of the Royal Meteorological Society, 106, 85-100, DOI 10.1002/qj.49710644707, 1980.

Wutzler, T., Lucas-Moffat, A., Migliavacca, M., Knauer, J., Sickel, K., Sigut, L., Menzer, O., and Reichstein, M.: Basic and extensible post-processing of eddy covariance flux data with REddyProc, Biogeosciences, 15, 5015-5030, 10.5194/bg-15-5015-2018, 2018.

Xu, B., Arain, M. A., Black, T. A., Law, B. E., Pastorello, G. Z., and Chu, H. S.: Seasonal variability of forest sensitivity to heat and drought stresses: A synthesis based on carbon fluxes from North American forest ecosystems, Global Change Biology, 26, 901-918, 10.1111/gcb.14843, 2020.

Yao, Y., Liu, Y. X., Zhou, S., Song, J. X., and Fu, B. J.: Soil moisture determines the recovery time of ecosystems from drought, Global Change Biology, 29, 3562-3574, 10.1111/gcb.16620, 2023.

Zheng, P. F., Wang, D. D., Yu, X. X., Jia, G. D., Liu, Z. Q., Wang, Y. S., and Zhang, Y. G.: Effects of drought and rainfall events on soil autotrophic respiration and heterotrophic respiration, Agriculture Ecosystems & Environment, 308, ARTN 107267, 10.1016/j.agee.2020.107267, 2021.

Zhou, S., Williams, A. P., Berg, A. M., Cook, B. I., Zhang, Y., Hagemann, S., Lorenz, R., Seneviratne, S. I., and Gentine, P.: Land-atmosphere feedbacks exacerbate concurrent soil drought and atmospheric aridity, Proceedings of the National Academy of Sciences of the United States of America, 116, 18848-18853, 10.1073/pnas.1904955116, 2019.